

PARTICLE LIFETIMES AND NEUTRINO CONSTRAINTS ON ULTRAVIOLET THEORIES

A Dissertation

Presented to the Faculty of the Graduate School
of Cornell University

in Partial Fulfillment of the Requirements for the Degree of
Doctor of Philosophy

by

Itay Nachshon

January 2013

© 2013 Itay Nachshon
ALL RIGHTS RESERVED

PARTICLE LIFETIMES AND NEUTRINO CONSTRAINTS ON
ULTRAVIOLET THEORIES

Itay Nachshon, Ph.D.
Cornell University 2013

In order to help the search for new physics we propose two methods for relating experimental results to theories. First, measurements of lifetimes can be done in two ways. For very short lived particles, the width can be measured. For long lived ones, the lifetime can be directly measured, for example, using a displaced vertex. Practically, the lifetime cannot be extracted for particles with intermediate lifetimes. We show that for such cases information about the lifetime can be extracted for heavy colored particles that can be produced with known polarization assuming we can measure their spin. Second, neutrino oscillation experiments are known to be sensitive to Non-Standard Interactions (NSIs). We extend the NSI formalism to include one-loop effects. We show how the parameters that can be extracted from the experiments are obtained from various loop amplitudes, which include vertex corrections, wave function renormalizations, mass corrections as well as box diagrams. We argue that the size of one-loop NSIs can be large enough to be probed in future neutrino oscillation experiments.

BIOGRAPHICAL SKETCH

Itay was born in Haifa, Israel, on December 14, 1978 to Vered and Yehuda Nachshon and is the younger brother of his sister, Sagit Prince. At age 12 his family moved to Timrat, Israel (25 Km. out of Haifa). His mother, Vered Nachshon, passed away when he was 15 at 1994 from melanoma.

Itay always liked physics and would do well in his physics studies and joined many physics clubs. He graduated from Nahalal High school at 1997 and joined the IDF from the mandatory military service in Israel. He was assigned as a programmer for the IAF for six years and was honorably discharged at 2003.

Following his service, he started his undergraduate studies at the Technion - Israel Institute of Technology in physics. He enjoyed his studies taking a broad range of course work in different types of physics: statistical mechanics, optics, low temperature physics, and particle physics. He enjoyed the excellent instruction from professors at the Technion including with Yael Shadmi, Gad Eilam, Moshe Moshe, Oren Bergman, Yoram Rosen, Shlomit Terem, Josef Avron, Ari Laor and many more. Itay married to Calanit Nachshon on June 2007.

Itay met his graduate advisor, Yuval Grossman, at the Technion taking a course in Introduction to Particle Physics which Yuval taught. Itay was immediately fascinated with beauty of the field of high energy phenomenology. At 2006 Itay graduated as a Bachelor of Science from the Technion, summa cum laude.

Following his graduation he began graduate studies at the Technion seeking to work in the field of high energy particle physics. He started working with Yuval Grossman beginning his first project. Yuval decided to move to Cornell University at 2007 and Itay, wanting to keep working with Yuval, moved with him. Itay continued his studies with Yuval Grossman until 2012 when he graduates from the PhD program.

This document is dedicated to my late mother, Vered Nachshon. It is also dedicated to my wife, Calanit Nachshon who supports me while I persuade my interests in physics.

ACKNOWLEDGEMENTS

I want to thank my family. My father Yehuda who never fails to try and look after me and help me. My late mother Vered who loved for me like only a mother could. My sister Sagit and her family, Tal, Shir, Roni, and Ori for their love and support.

I also thank my wife Calanit for supporting me during my studies at Cornell. Your support, companionship, and love make my day and carried me on. I love you.

Thank you Yuval Grossman for always helping me through and doing the most to help me grow. Your kindness is a great asset to your students. Physics conversation and classes with you have helped me greatly and advanced my understanding of physics.

Thank you Brando Bellazzini and Paride Paradisi for being great collaborators and making our work excellent.

Thank you Csaba and Peter for taking the time to teach me and support my academic studies at Cornell.

Thank you Csaba, Maxim, Yuval, Liam, and everyone on the particle theory group for teaching me how to think about problems and how to approach them. For advancing my understanding of physics and being companions to the fascination with physics.

I thank my friends both in Cornell and outside of Cornell in the USA and in Israel. It is a wonderful thing to have caring friends as we go through life.

TABLE OF CONTENTS

Biographical Sketch	iii
Dedication	iv
Acknowledgements	v
Table of Contents	vi
List of Figures	viii
1 Introduction	1
1.1 High energy physics and the properties of fields	1
1.2 The case for new physics at the weak and TeV scale	5
1.3 Lifetime determination	7
1.4 Relating experiments to UV theories	11
1.5 Theories beyond the standard model and the neutrino sector . . .	14
2 Determining Lifetimes using spin information	17
2.1 Introduction	18
2.2 Formalism	21
2.3 A more realistic scenario	25
2.4 Discussions and conclusions	31
3 Matching Neutrino sector IR operators to BSM UV theories	33
3.1 Introduction	34
3.2 Notations and formalism	36
3.3 One loop NSI	40
3.3.1 Correction to the W exchange amplitude	40
3.3.2 Non-universal effects	45
3.3.3 Matter effects	46
3.3.4 Scalar charged current	48
3.4 One loop NSIs and Supersymmetry	53
3.4.1 $V - A$ charged current	53
3.4.2 Scalar charged current	59
3.4.3 Numerical analysis	62
3.5 Discussion and conclusion	66
A Detailed for lifetimes via spin information calculation	67
A.1 Calculation of spin information being lost through mixing	68
A.1.1 Assumptions	68
A.1.2 spin information lost in mixing and vector meson decay .	69
A.2 Spin information in the top quark decay	71

B	Details for matching UV BSM theories with IR Neutrino sector operators	73
B.1	Self-energies and vertex correction in the MSSM	74
B.2	How self energy and vertex correction enter the theory	76
B.3	Detailed calculation in a simplified model	79
B.3.1	loop correction for the kinetic term	79
B.3.2	loop correction for the interaction vertex	81

LIST OF FIGURES

2.1	r as a function of Γ^{-1} (in MeV^{-1}). We use Eq. (2.13) setting $\Delta m = 1 \text{ MeV}$ and $\Delta\Gamma = \Gamma_\gamma = 1 \text{ eV}$	25
3.1	1-loop contributions to the lepton self-energies (left) and to the vertex (right). The virtual particles running in the loop are sleptons and a neutralino.	55
3.2	A contribution to the effective $\bar{\nu}_\tau \ell_R H^+$ coupling.	60
3.3	Left: NSIs in the process $K \rightarrow \ell \nu$ induced by Higgs mediated effects. Right: NSIs in the process $\mu \rightarrow e \nu \bar{\nu}$ induced by W -penguin and gaugino/slepton boxes. See the text for details.	64

CHAPTER 1

INTRODUCTION

1.1 High energy physics and the properties of fields

In physics we would like to understand what the universe is made of. Historically this gave rise to ideas like the atom and atomic physics, nuclear physics, subnuclear physics, as well as quantum mechanics, relativity, quantum field theory and much more. This question is in the heart of physics and the scientific endeavor. Basic human curiosity leads inevitably to searching for the basic building blocks of nature.

Early on in this pursuit physicists came to a deep and nontrivial understanding. The rules of nature are not invariant relative to the scale of the problem. This means that there are preferred scales in nature like the masses of particles and Λ_{QCD} . Therefore physics at different scales is also very different. From the scale we live in to the atomic scale to the nuclear scale and the subnuclear scale all the way to the weak scale there was always a new set of rules of nature.

In other words at larger scales we can probe and find different physics rules derived from more fundamental rules at lower scales. This breaking of scale symmetry also means we cannot always derive the more fundamental theory from a large scale theory (e.g. nuclear theory from atomic theory or high energy particle physics from nuclear theory). On the other hand large scale physics can provide hints to lower scale physics. In this document we will call the new high scale physics at or above the weak scale, the UV physics. We will also call the standard model and low scale neutrino physics, the IR physics. For example the

weak scale can be deduced from weak interactions. If we understand that this four fermi interaction comes from a higher dimensional operator we can deduce the weak scale (assuming the strength of the interaction at the weak scale is not weak). This gives rise to searching for UV physics, though processes affecting the IR physics, that cannot come from IR physics. This avenue to discovery has been quite fruitful in processes like weak interactions as well as in giving bounds that can restrict UV physics.

Physicist understood that quantum mechanics plays an active role in breaking scale invariance. The running of parameters is effected by quantum loops. Also zero point energy arises in confining theories (proton mass) as well as non-confining theories (the Rydberg constant) giving rise to scales in the theories. Further exploration showed the important rule of relevant and non-relevant operators. (Relevant operators in the UV theory and non-relevant operators as important hints to the UV theory).

Because physics is not invariant to scale it affects the way we try to find the building blocks of the universe. We cannot do that by looking at larger scales, we have to do this by looking at smaller scales. The few exceptions to that rule: Cosmology, where at the big bang, cosmological events were effected by small scale (high energy and high temperature) physics; IR physics affected by non-relevant operators like rare decays at the atomic scale where the symmetries of the larger scale physics forbid processes that smaller scale physics allows.

Looking for smaller length interval scales to find more fundamental physics, we need to probe for higher momenta because of the Heisenberg uncertainty principle for momentum and length intervals. To achieve higher momenta we need higher energy particles. Therefore we can quantify the scale we probe by

the energy available. This leads to the need for collider physics where we accelerate particles to high energy and try to probe the outcome of these collisions. The idea is to observe processes and decays of elementary particles at higher energy scales which relates through the principle above to small scales.

Another approach is to look at lower energy experiments for processes that are forbidden by the lower energy theories. If a higher energy theory allows these processes then for a short time the degrees of freedom in the experiment can tunnel through higher energy states. This is a consequence of the Heisenberg uncertainty principle for energy and time intervals.

In this approach we have few options. Because the lower energy theory can predict that some processes are forbidden then any signal would mean new physics. We can also try to calculate to a very high accuracy quantities at the IR theory and so any deviation from the predictions would hint at UV contributions. Such is the case with the measurement and calculation of $g - 2$. It is important to note that in searching for processes forbidden by IR physics we can also look for new relevant operators (and not just irrelevant ones). We will see that in neutrino physics the marginal operators coming from UV theory loops are interesting. Even though we produce effective marginal operators, they are small and so just like the usual case with the non-relevant operators, their contribution is small.

In field theory we are looking for new fields with new interactions at higher energy scales. Relativity and more specifically Lorentz and Poincaré Invariance teaches us that there are only few properties that are fundamental to a new particle. The mass of the particle, the representation of the particle (spin), the decay time of the particle, as well as what are the interaction coefficients for any

Lorentz invariant vertex. This includes the representation in new fundamental force (charges), Yukawa interactions, scalar interaction, and for the case of rare decays, higher dimensional operators. Therefore from the experimental point of view these are the things to measure in the search for elementary physics.

Therefore in the search for new particles, after finding a new particle resonance or access or a decay with an interesting geometry, we will need to find the mass, spin, lifetime, and interactions of the intermediate particles. In the case of a resonance the energy of the peak will tell us the mass, and the energy width will usually tell us the decay time (unless the decay is long). The specific interaction can be deduced from the branching ratios and the spin can be deduced from the spin of the daughter particles and the angular distribution of the decay.

Another scenario is when the particle is in a decay chain. In that case we may be able to find its mass using methods such as MT_2 and we may find the spin of the particle using the angular distribution between the sister and daughter particles.

Much work has been done to understand how colliders can determine properties such a mass, spin and lifetimes of particles. The current list of suggested methods allows for measurements of particles from a large classes of proposed theories. Still there are many proposed models where mass, spin and lifetime measurements cannot be done or cannot be done easily for the predicted particles. These measurement can sometimes be crucial to ruling out competing models.

1.2 The case for new physics at the weak and TeV scale

Before getting more specific with the details of this thesis let us examine why we think there is new physics between the weak and TeV scale. Since the reach of the LHC is a few TeV we need to remember the reasons we are looking at these scales.

Since we talked about scale being broken we can bring up this point here. In the history of physics there simply was never a case of a scale with no interesting physics. Even if we found in experiment, physics that is not motivated by trying to solve a theoretical question that would not be surprising. Often new physics showed up at every scale. This was the case for the mass of all the particles in the standard model which showed up at every energy scale until the weak scale. That was also the case in atomic and nuclear physics.

At the point of writing this thesis the Higgs boson has already been found. There is no reason to assume the Higgs is the plain standard model version. We could have a doublet or we could have a more complex structure. Now that we have found the Higgs boson we need to probe this sector further and see if we can find interesting structure there.

This raises the strongest case of TeV physics. The topic of how to stabilize the mass of the Higgs boson. If we allow the UV physics to be at a much higher scale than the weak scale, quantum fluctuation in a natural theory (in the running of the Higgs mass) should push the Higgs mass to the scale of that UV theory. This is the result of having the mass of the Higgs as a relevant two dimensional operator in the theory (as opposed to a marginal operator). The mass of the Higgs then run quadratically with the cutoff scale (or the scale of the UV theory).

Therefore some new physics should show up just above the weak scale and stabilize the Higgs mass.

Theories have been proposed that put that new physics at the TeV scale in a way that the correction to the Higgs mass is natural and sometimes hide the new physics in a way that is hard for the collider experiments to find. The argument of naturalness is also not very precise. For example, would anyone object if nature happened to have chosen to be in a theory where percent level accuracy in correction to quantum fluctuations is needed? With all that said, however, it puts a strain on the theory to try and hide the theory up to the TeV and stabilize the mass of the Higgs at the same time. If we just go with what is simple this mechanism seems to indicate that there must be new physics somewhere up to the TeV scale.

Finally, we have dark matter. If we take the usual story of the big bang and assume that dark matter is created with enough time to come to equilibrium (before the universe cools off), and further assume weak coproduction of dark matter then the mass scale of the dark matter should be at the weak scale. There are a lot of assumptions here. For example, if we change the interaction from weak interaction to something weaker we can make the mass of the dark matter particles smaller. Alternatively, we can also change the way dark matter is produced to out of equilibrium processes. This is not a strong argument but can be given as an added hint for weak scale physics.

1.3 Lifetime determination

There are two main methods for lifetime determination at colliders. One way is to try to see the width of a resonance then by the uncertainty principle this indicates the lifetime of the particle. Therefore, after gathering enough decays we can find the width directly. Then, by the uncertainty principle the lifetime $t_{\text{lifetime}} = \hbar/\Gamma$. This is also very useful if we consider certain particles can decay in invisible modes. Then, even if we don't see some modes we can deduce that something is missing since the branching ratios would not add up.

The other method for long lived particles is measuring a displaced vertex of the decay. By knowing how fast the particle traveled (usually close to the speed of light) we can deduce how long the particles lived. Therefore, by gathering enough statistics we can find the lifetime of the particle. The other way in which this is useful is that we know exactly what the particle decayed into since we only consider tracks that lead to the secondary decay vertex.

An extreme but very possible case of long lived particles would be new particles that leave the collider without decaying. People speculated they may be able to trap these particles or maybe some QCD or QED charged particles will get lodged in the atoms and nucleus and decay later. This means that all we need to do is to wait for decays after the collider stopped working.

As we will see in the first part of this thesis, this leaves a wide range of lifetimes that we cannot measure between measuring the decay width to displaced vertices. We will also see that there are theories that can produce particles at these ranges. The usual paradigm in these cases is that we are out of luck and cannot measure the lifetimes of these particles. We will see below that in fact there is

an indirect way that works for these cases.

To understand how we would go about measuring lifetime indirectly we must first look at spin determination. The usual way to do this is to look for angular distribution of daughter particles coming from the decay. The angular distribution of daughter particles (and sometimes particles created with the intermediate particle, i.e. sister particles) is related to the spin of the particles in question because of angular momentum conservation. In the search to determine the spin of particles many methods were suggested that all help determine spin for a wide variety of scenarios.

For example, we can look at the angular correlation between the sister particle and a daughter particle. This can include two body decays like into a t, \bar{t} where the correlation between the \bar{t} momenta and the daughter particles of the t give an angular distribution. Another example is in a chain decay between the sister outgoing particle and a daughter one step down the decay chain. We can also find correlation in three body decays.

In order to understand the relevance of spin information to lifetime determination of particles, we can use an analogy from the hyperfine splitting of the hydrogen atom. In the Hydrogen atom the (electromagnetic) spin interaction between the proton and the electron leads to a splitting of the ground state into a state where the two spins make a scalar, $(|\uparrow\downarrow\rangle - |\downarrow\uparrow\rangle) / \sqrt{2}$, and a state where the two spins add up to a vector, $|\uparrow\uparrow\rangle, |\downarrow\downarrow\rangle, (|\uparrow\downarrow\rangle + |\downarrow\uparrow\rangle) / \sqrt{2}$. The energy difference of the two states is proportional to E^2/M_p . Here E is the available energy in the state (in this case the zero point energy of the ground state) and M_p is the mass of the proton.

Therefore, if you produce a mixed state of a scalar and a vector Hydrogen atom then the spin of the proton will go through Rabi oscillation between the scalar and $m = 0$ vector state. $m = \pm 1$ vector states will not participate in the oscillation resulting in some of the spin information preserved. That will go on until the part of the state which is a vector will decay to a scalar resulting in the hydrogen 21 cm line. In relation to our previous arguments the energy of the hydrogen line is small because the mass of the proton is much greater than the available energy.

A classical way to understand this is to consider that the two spins produce magnetic fields and a heavy charged particle will oscillate in a magnetic field at a rate inversely proportional to its mass. Therefore, in the quantum mechanical scenario the relevant energy scale of the proton spin oscillation is proportional to energy splitting between the two states which is proportional to the inverse of the proton mass. In our case we will find that both the mass splitting, and the decay time of the vector state, produce energy scales relevant to the determination of the lifetimes of particles.

The analogy described above is carried to heavy mesons. Electromagnetism is replaced with QCD and the interaction is between the heavy quark and the light spectator. The spin of the heavy quark will undergo spin oscillation between the scalar state and the $m = 0$ state. This is just like the Rabi oscillations in the hyperfine splitting scenario where the oscillation frequency is proportional to the mass splitting between the scalar and vector mesons. The vector $m = \pm 1$ states will not participate in the oscillation resulting in some spin information being conserved. The vector meson will eventually decay into the scalar meson emitting a photon. This photon will not be observed since it has energy at the

mass splitting energy which is much smaller than what can be observed at the collider environment. Thus, when the vector meson decays all spin information is lost.

We have two scales of interest. The first is the mass splitting between the scalar and vector heavy mesons. If a weak decay of the heavy quark occurs before this scale, then all the spin information is preserved. If the weak decay of the heavy quark occurs after this mass scale, then it decays as it oscillates and some of the spin information is lost because the top decays in a mixture of up and down spins. The portion of the spin information in the $m = \pm 1$ vector states will be preserved. By looking at the fraction of the spin information lost, we can find if the weak decay of the heavy quark happened before or after the mass splitting scale.

Finally, if the decay time is longer than the decay of the vector to the scalar meson, then a photon we cannot detect is emitted carrying all the angular momentum information. As a result, the decay products of the scalar meson give an isotropic angular distribution. If no spin information is observed and we are confident that all other mechanisms of spin information loss are accounted for, then we know that the weak decay of the heavy quark is longer than the vector meson decay time.

This means that how much spin information is measured relative to what is expected give us a handle of how long the heavy quark lives. This method can be extended to any heavy QCD charged particle provided its spin and the spectators spin do not create trivial representations and provided we can use an effective field theory like heavy quark chiral effective field theory to determine the mass splitting and the decay of the higher spin representations.

If for example we are talking about a heavy baryon then the two light quarks will make a scalar state. This is because there is nothing protecting the mass splitting of the vector state of the two light quarks. Therefore, it will be at a much higher energy scale and not produced. Another example where this method cannot work is squarks in super symmetry. Since their spin is zero we expect no mass splitting for scalar and vector states. Examples when it could work are KK modes of quarks (with scalar and vector state mesons) or gluino glue balls (with spin 0,1,2 meson states).

In order to be able to find the mass splitting and the decay time of vector and higher representation states, we need to make a new heavy particle chiral effective field theory. In principle that is not difficult. The problem is that any effective field theory would need to have its counter terms measured. For heavy quark chiral effective field theory we have the D and B meson. Here we would need more than one meson or we could count on lattice QCD by inserting a new particle at the energy levels where it is possible to do a calculation and then run the theory up to the energy scales of our new particle.

1.4 Relating experiments to UV theories

Usually, experimental result in high energy theory come in specific forms. Results from colliders can come through the discovery of new particles at which case we find its mass, spin, and decay branching ratios. We can also look for the excess of different processes. For example, we can search in various inclusive processes, we can search process that we do not expect to see from the standard model or that have a specific decay topology that we believe will be indicative

of specific theories. In general, we can classify these methods by how generic they are with respect to proposed theories versus how much we are searching for very specific things we can calculate.

Various proposed models come with signals which are specific to them. For example, we can look for a specific topology or we can search for processes that have a very nice and clean signal. Therefore, we can search for models by looking for these specific signals. This leaves us with a shopping list of signals and proposed theories. Although this method is useful there is no guarantee nature would pick one of the theories physicists like.

More inclusive methods include searching for general excess in standard model production rates. This is because we did not specify with UV theory we are looking for. For example, we can also look sometimes at processes with a very high predicted rate if we know we can calculate and measure the rate to a high precision. Processes like inclusive QCD production as well as production rates with different jet multiplicity are such processes.

One method that allows to search in a more generic way is searching for rare processes at the IR (i.e. processes that are forbidden by the standard model). We can take a process that is excluded by the standard model or has a very small predicted rate and see if we can find a rate greater than predicted. Because we did not specify the UV theory we only know we have a process measured at the IR that is not accounted for by the standard model. It is possible to construct a UV theory that does not produce the desired operators but this provides us with a handle to exclude UV theories or if we find a rare process to constrain what a possible theory may be.

UV theories come with a variety of parameters. In order to calculate a branching ratio or decay rate of a process we usually need more than a few of these parameters. Usually the UV and IR degrees of freedom will not line up. In order to predict a high dimensional operator from a UV theory we need Feynman diagrams in the UV theory that carry many of the UV parameters. This makes it difficult to invert the process. What we would really like to know is, given a discovery of some rare process or decay, what does it say about UV theories, which are excluded and which are safe. In a theory with many parameters this could mean that certain regions in a multidimensional parameter space would be excluded and some areas would be allowed.

Thus, we need generic ways to relate UV theories to IR results. This will allow us to easily come to a conclusion about the UV theories. To evade IR bounds many ways have been proposed for various cases. For example, much work has been done on models that respect the flavor structure of the standard model. Also, all UV theories accommodate the electroweak precision measurements. Therefore, if new IR bounds arise this will mean constraining the UV theories further. On the other hand, weak interactions can be brought as an example for how fruitful finding an IR effective operator (four Fermi interaction) can be.

More recently simplified models have been suggested as a way to relate collider results to super symmetry. As will be discussed below new high luminosity experiments in neutrino physics promise to provide a new IR window to the exploration of UV theories. Previously the difficulty in detecting neutrinos meant we could not look for rare interactions in the neutrino sector.

1.5 Theories beyond the standard model and the neutrino sector

New high luminosity experiments in the neutrino sector provide new and exciting prospects. The next generation of long baseline experiments will provide a more accurate measurement of the mixing parameters. The new precision provides new opportunities to measure rare processes in the neutrino sector other than oscillations.

Oscillations are proportional to the length of the experiment and new processes from higher dimensional operators will not in general be proportional of the length of the experiment. This means that we can distinguish between oscillations and higher dimensional operators. By placing a detector next to the source we can probe neutrinos that were just created and did not have time to oscillate. Therefore, if the mixture of these neutrinos is different from what we expect in the standard model production, then we know that they come from rare lepton number violating decays and interactions with the detector.

There is another mechanism here that is worth mentioning. Usually, we expect to have a process proportional to the square of the amplitude. Here, because there is a tree level process (neutrino oscillations), then the dominant contribution would come from the interference term between the oscillations and the rare decay. This is what is called a square root enhancement. If the tree level effect was small we would not be able to see this effect.

These experiments give us a new way to probe UV theories based on the neutrino sector. To be able to come to conclusions, we need to demonstrate that

experimental result in the IR could be related to UV theories in a generic way. We need to produce effective operators in a generic way and then relate those operators to the experimental results. Then, one can invert this process and find how the experimental results constrain the parameter space of the theory. The idea is to create a generic way to calculate this correction. Given a UV theory we show how to find the IR operator in a robust way.

In this way we can have a new theory independent way of probing UV theories in a way that was not done yet. Theories proposed up until today such, as super symmetry, did not take the neutrino sector into consideration. The theories were not constrained in the same way they were for electroweak precision measurements or flavor. There are some exceptions to that. For example, in theories like super symmetry, we have to take into consideration $\mu \rightarrow e \gamma$. The loops that can produce this process can also produce weak interaction to different types of neutrino. Here the square root enhancement comes to our aid. The $\mu \rightarrow e \gamma$ does not have a standard model tree level process, so there is no interference term. On the other hand, the neutrino sector does have oscillation as a tree level process.

Another observation we will see in the work below is that if the electroweak theory is not broken, then the kinetic loop corrections align exactly with the interaction term loop correction, keeping the derivative covariant. Thus, these corrections to the weak interaction have to be proportional to the electroweak symmetry breaking scale. This is not true for the charged Higgs interaction. This is because this interaction does not belong to a covariant derivative.

The next decade will provide new and exciting windows into physics at smaller scales. The LHC will probe and is probing the content of nature at the

TeV scale. New IR experiments, such as long baseline neutrino experiments, will constrain the theory further from the IR or find effects of the UV theory on the IR. These exciting new developments in experimental high energy physics mean theorists need to be prepared for data coming out of these experiments.

CHAPTER 2
DETERMINING LIFETIMES USING SPIN INFORMATION

Based on the 2008 article “Hadronization, spin, and lifetimes,” written in collaboration with Yuval Grossman and published in JHEP **0807**, 016 (2008).

2.1 Introduction

There are strong motivations to hope that the LHC will find new particles with electroweak scale masses. Once such a new particle is discovered, the first task will be to determine its properties, in particular, mass, charges, spin and lifetime. Clearly, such determinations require much larger statistics than what is needed for discoveries of new states. The hope is that eventually, with enough data from the LHC and future machines, we will be able to determine these properties for all the new particles.

In this work we concentrate on determining lifetimes. There are basically two ways the lifetime of a particle can be determined. The first is to directly measure its width. This method works when the intrinsic width is larger than the experimental resolution. The experimental sensitivity depends on many factors, like the mass of the particle and its charge. Very roughly, for a particle with mass of a few hundred GeV, its width can be extracted when $\Gamma \gtrsim 1$ GeV. The other method to extract lifetimes is by looking for a displaced secondary vertex. This can be done, very roughly, for $\tau \gtrsim 1$ ps, that is, $\Gamma \lesssim 10^{-4}$ eV. We see that there is a very large window,

$$10^9 \text{ eV} \gtrsim \Gamma \gtrsim 10^{-4} \text{ eV}, \quad (2.1)$$

which we denote as “the problematic region,” where lifetimes cannot be extracted.

The fact that our ability to measure lifetimes is limited may not be a problem. For example, in a generic SUSY model we expect the LSP to be stable and all other super-particles to have widths that are larger than 1 GeV. This is the generic case in most available models of physics beyond the SM; the unstable

particles are very short lived while other new particles are stable due to an exact symmetry. There are, however, exceptions. There are well motivated models with new, unstable particles with lifetimes that are much longer than the naive ones, such that their widths are within the problematic region. This is the case, for example, in Z' -mediated SUSY Breaking [?] (for the gluino and the NLSP Wino), in split SUSY [?] (for the gluino when $m_s \lesssim 1000$ TeV) and in GUTs in warped extra dimension [?, ?] (for the GUT partners).

Below we describe a way that, in principle, can tell us information about a lifetime of a particle in the problematic region. The basic idea is as follows. Consider a particle of mass m that is not a singlet of $SU(3)_C$ nor of the Lorentz group. Thus, if its lifetime is longer than the QCD scale, it hadronizes before it decays. If the particle is produced polarized, the fact that it hadronizes could eventually reduce its initial polarization. In cases where the polarization can be measured and compared to the expected one, we can extract the amount of depolarization. Knowing the time scale associated with the loss of polarization, makes it possible to determine if the lifetime is larger or smaller than that time scale.

The loss of polarization takes place at time scales much longer than the hadronization scale [?]. The typical time for hadronization is Λ_{QCD}^{-1} while for depolarization it is $m\Lambda_{QCD}^{-2}$. This is similar to the case of the hydrogen atom. The energy scale associated with depolarization of the heavy proton is that of the hyperfine splitting and it is suppressed by m_e/m_p . In particle physics terms, the fact that the depolarization time scale is long is a manifestation of the heavy quark spin symmetry. In the $m \rightarrow \infty$ limit the spin of the heavy quark is conserved. Thus, it can be changed only on time scales that are associated with

energy scales that are suppressed by at least $1/m$.

In fact, the loss of polarization occurs in several stages. Thus, a more refined knowledge about the lifetime can be obtained. For the purpose of illustration we consider a world where the top quark has a long lifetime. We neglect hadronization into baryons, and consider the two lightest top-mesons, T^* and T (the analog of B^* and B). These two states form a doublet under the heavy quark spin symmetry [?]. We further consider a very clean environment where we know the initial top polarization. Then, the angular distribution of the decay products can be used to measure the top polarization. Depolarization effects caused by the fact that the top hadronizes, make the final polarization smaller than that of a free quark.

There are several time scales associated with hadronization and depolarization [?]:

1. $t_1^{-1} \sim \Lambda_{QCD}$: This is the time scale where hadronization occurs. That is, after that time the top quark is hadronized into a heavy hadron, which can be a superposition of T and T^* , and possibly many light hadrons. (There is a small probability to hadronized into a top baryon, which we neglect for now.) Since the mass difference between T and T^* is much smaller than Λ_{QCD} , the meson containing the top quark is not in a mass eigenstate but rather a coherent superposition of T and T^* .
2. $t_2^{-1} \sim \Delta m$: The next relevant time scale is that associated with the splitting between the two hadrons

$$\Delta m \equiv m(T^*) - m(T). \tag{2.2}$$

At this time the system starts to “feel” the mass difference between the two

hadrons. The system oscillates between the two mass eigenstates, which practically means loss of coherence. t_2 is the time scale that controls the first depolarization stage.¹ As we show below, at times much larger than t_2 , half of the initial polarization is lost.

3. $t_3^{-1} \sim \Gamma_\gamma$: The last relevant time scale is the one that controls the $T^* \rightarrow T$ transition

$$\Gamma_\gamma \equiv \Gamma(T^* \rightarrow T\gamma). \quad (2.3)$$

Since the T is a scalar, once the T^* decay into a T , all the initial polarization information is lost.

By measuring the amount of depolarization we can get a rough idea about the width of the top quark, Γ . If no depolarization occurs, we know that $\Gamma \gg \Delta m$. If half of the polarization get lost, it implies that $\Gamma_\gamma \ll \Gamma \ll \Delta m$. All the initial polarization is lost when $\Gamma \ll \Gamma_\gamma$.

2.2 Formalism

We develop the formalism by considering a simple toy model. We comment about more realistic scenarios later, but a full study of a realistic model is left for future work.

Our toy model consists of a heavy “top” quark, t , a massless “bottom” quark, b , and a massless scalar, ϕ . That is, the t and the b are spin 1/2 fermions that transform as 3 under $SU(3)_C$ while ϕ is a scalar and does not carry color. The

¹It is often said that “the top keeps its spin since it decays before it hadronizes.” While this statement is correct, it is misleading. The relevant time scale for depolarization is much longer than the hadronization time scale.

interaction term is chiral

$$y_{tb} \bar{t} \frac{1 - \gamma_5}{2} b \phi. \quad (2.4)$$

We assume that the top is produced fully polarized and that we know its spin direction, which we denote as the z axis. We further take m_t to be known and to be of order a few hundred GeV. In this simple model we can measure the final top polarization by the angular dependence of the out going b quark

$$\frac{d\Gamma}{d \cos \theta} = \frac{m_t y_{tb}^2}{64\pi^2} (1 - 2 \langle s_z \rangle \cos \theta). \quad (2.5)$$

Here θ is the standard azimuthal angle and the normalization is such that a polarized top has $\langle s_z \rangle = 1/2$.

We emphasize that the angular distribution of the decay products depends on the spin of the top quark even after hadronization. It is a very good approximation to neglect spectator effects in the decay. Thus, the spin of the hadron is irrelevant in the decay; it is only the spin of the heavy top that counts.

Once m_t is known, we can use heavy quark symmetry to calculate Δm and Γ_γ (the details of the calculations are given in the next section). Thus, we assume that the following quantities are known:

$$m_t, \quad \Delta m \equiv m(T^*) - m(T), \quad \Gamma_\gamma \equiv \Gamma(T^* \rightarrow T\gamma), \quad (2.6)$$

such that $m_t \gg \Delta m \gg \Gamma_\gamma$. In general, Γ_γ carries a flavor index, as it depends on the light quark. Here we further simplify by assuming that the t quark has only one way to hadronize, say into a T_d meson, and thus we omitted the flavor index. To a very good approximation both Δm and Γ , the weak decay rate of the top, are independent of the light degrees of freedom. Therefore, Γ_γ is also the width difference between the two mesons,

$$\Delta\Gamma \equiv \Gamma(T^*) - \Gamma(T) = \Gamma_\gamma. \quad (2.7)$$

It is useful to define two bases that describe the state of the heavy meson. The mass basis is spanned by the T^* and T mesons. In this basis the total spin and the total spin in the z direction are known. The spin basis is the one that is labeled by s_Z of both the top and the spectator d quark. We denote its eigenvectors by $|s_t, s_d\rangle$ with $s_t, s_d = +, -$. The relation between the two bases is

$$\begin{aligned} T^*(1, 1) &= |++\rangle, & T^*(1, 0) &= \frac{|-+\rangle + |+-\rangle}{\sqrt{2}}, \\ T^*(1, -1) &= |--\rangle, & T(0, 0) &= \frac{|-+\rangle - |+-\rangle}{\sqrt{2}}. \end{aligned} \quad (2.8)$$

Next we move to calculate $\langle s_Z \rangle(t)$, the top polarization as a function of time. We set $t = 0$ as the time the top is produced and hadronizes. That is, we neglect the stage of hadronization which is very fast. We assume that the top is produced with a spin in the z direction. We further assume that the light quark in the meson is unpolarized, that is, it has equal probability to have spin up or down. See [?] for discussion on that point. Thus, we can write the meson state $T(t)$ at time $t = 0$ as

$$T(t = 0) = \frac{|++\rangle + |+-\rangle}{\sqrt{2}} = \frac{T^*(1, 1)}{\sqrt{2}} + \frac{T^*(1, 0)}{2} + \frac{T(0, 0)}{2}. \quad (2.9)$$

Since we assume that Δm and $\Delta \Gamma$ are known we can get the time dependences of the meson state

$$T(t) = \frac{e^{-\Gamma t}}{2} \left[\sqrt{2} T^*(1, 1) + T^*(1, 0) + \exp[(i\Delta m + \Delta \Gamma)t] T(0, 0) \right], \quad (2.10)$$

where we omit an irrelevant overall time dependent phase. Using Eq. (2.10) we can get the time dependence of the top spin. That is, assuming we have a top with spin up at $t = 0$ the probability to find the top with spin up at a later time is

$$\frac{\langle s_Z \rangle(t)}{\langle s_Z \rangle(t = 0)} = \frac{e^{-\Gamma t}}{2} \left(\cos(\Delta m t) + e^{-\Delta \Gamma t} \right). \quad (2.11)$$

A few points are in order regarding Eq. (2.11):

1. At very short times, $t \ll 1/\Delta m$, the polarization is unchanged from its initial value.
2. At later times, $1/\Delta\Gamma \gg t \gg 1/\Delta m$ the oscillatory term is averaged to zero and we see that the polarization reduced to half its initial value. This result can be understood from the meson picture. At $t = 0$ the $T^*(1, 0)$ and $T(0, 0)$ are in a coherent state. At later times, $t \gg 1/\Delta m$, the state is effectively a decoherent sum of these two states, each with an average zero top polarization. The $T^*(1, 1)$ state, however, stays polarized, and thus half of the original polarization is maintained.
3. At very long times, $t \gg 1/\Delta\Gamma$, when the $T^* \rightarrow T\gamma$ decay takes place, there is complete depolarization.

Since in practice the time evolution of the meson cannot be traced, we have to integrate Eq. (2.11) over time to get the average polarization. We define $\langle s_Z \rangle^{free}(t)$ to be the average top polarization assuming no hadronization. (The time dependence of $\langle s_Z \rangle^{free}(t)$ is a trivial exponential decay.) We parametrize the amount of integrated remnant top polarization by

$$r \equiv \frac{\int dt \langle s_Z \rangle(t)}{\int dt \langle s_Z \rangle^{free}(t)}, \quad (2.12)$$

such that $r = 1$ indicates that the initial polarization is maintained while $r = 0$ refers to a case that the top decayed after it was completely depolarized. We find

$$r = \frac{1}{2} \left(\frac{1}{1+x^2} + \frac{1}{1+y} \right), \quad (2.13)$$

where we defined

$$x \equiv \frac{\Delta m}{\Gamma}, \quad y \equiv \frac{\Delta\Gamma}{2\Gamma}. \quad (2.14)$$

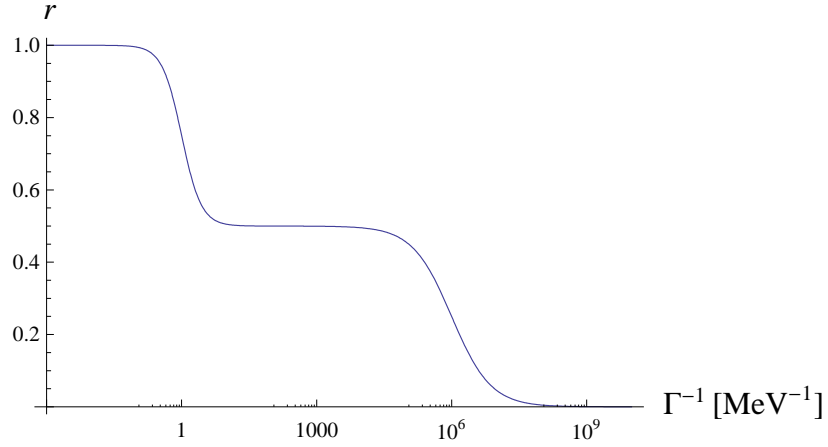


Figure 2.1: r as a function of Γ^{-1} (in MeV^{-1}). We use Eq. (2.13) setting $\Delta m = 1 \text{ MeV}$ and $\Delta\Gamma = \Gamma_\gamma = 1 \text{ eV}$.

Eq. (2.13) is the main result of this Section. It demonstrates how we can get information about the width of the top, Γ . In principle, by measuring r and using Δm and $\Delta\Gamma$ as inputs, we get Γ precisely using Eq. (2.13). This is illustrated in Fig. 2.1. In practice, however, the Γ dependence of r is strong only near $x \sim 1$ and $y \sim 1$. Far away from these regions Γ cannot be practically probed. This can be seen in Fig. 2.1 where far from $x \sim 1$ and $y \sim 1$, r is very flat.

2.3 A more realistic scenario

In order to make the lifetime probe realistic, the following points have to be addressed:

1. How well can we calculate the initial polarization?
2. How well can the polarization at the time of decay be measured?
3. The hadronization can be into a baryon or a meson, and each of them has

several different possibilities for the light degrees of freedom. How well do we know the flavor ratios after hadronization?

4. Given the mass, spin, and $SU(3)_C$ representation of the new heavy particle, how well can we calculate Δm and Γ_γ ?

Regarding the first point; the initial polarization can be calculated within any specific model. That is, if we have a model we put to test, in principle, we know the initial polarization. Clearly, the amount of theoretical uncertainty depends on how well the model parameters are known. Our hope is that by the time the ideas we propose can be used, the initial polarization can be determined to sufficiently high precision.

Moving to the second point; discussion of ways to measure heavy particles spin and polarization have been studied before, see, for example, Refs. [?, ?, ?], and for a recent review see [?]. The point is that these ideas can be carried out for the particles we are interested in.

Polarization measurements have been suggested (and used) to determine the spin of particles. To measure that, those methods do not have to be very sensitive to the accuracy of the measurement. To utilize them for our purpose, however, it is essential to have a good understanding of both experimental and theoretical errors. We have to address various questions, for example: Is the angular dependence being washed out by massive decay products? What is the chirality of the decay vertex [?]?

From now on we confine the discussion to the case of a spin 1/2 color triplet particle. We start by determining the flavor ratio after hadronization. Far from threshold it is reasonable to assume that the hadronization is independent of

the mass of the heavy quark. Thus, we can use b data in order to predict the hadronization for a heavy color triplet spin half. Isospin symmetry tells us that at high energy the probability to hadronized into T_u and T_d is about the same. In the B case the two other significant hadronization modes are into B_s and baryons. Using the data [?] it is straightforward to predict $P(X)$, the probability to hadronized into the hadron X , as

$$P(T_u) \approx 40\%, \quad P(T_d) \approx 40\%, \quad P(T_s) \approx 10\%, \quad P(\Lambda_t) \approx 10\%. \quad (2.15)$$

We use standard notation extended to the top case. That is, T_q is a meson made of t and \bar{q} quark, while Λ_t is a baryon made out of a t and two light quarks. Note that close to threshold the situation might be different as phase space effects can be important. In principle, such effects can be estimated.

Next we discuss the determination of Δm and Γ_γ . We start with the baryons. The lowest state, denoted by Λ_t , is a spin half. The two light degrees of freedom are in a relative spin zero configuration, and therefore Λ_t is a singlet of the heavy quark spin symmetry. Since the light degrees of freedom are in a spin zero configuration the spin of the baryon is the same as the spin of the heavy quark. Thus, the baryon keeps the initial polarization and hadronization effects are not important.²

The situation with the meson doublet, T and T^* , is more complicated. In the following we estimate Δm and $\Delta\Gamma$. The idea is to use D and B data and Heavy Quark Effective Theory (HQET) to predict these quantities for a heavy top.

²For the B case there is a subtlety related to the Σ_b that can actually affect the initial polarization. This issue is discussed in [?], where it is shown that the effects are important for the case of $m \sim 5 \text{ GeV}$ but can be safely neglected for heavy quarks with $m \gtrsim 100 \text{ GeV}$.

We start with the calculation of Δm . It is determined by the HQET λ_2 parameter [?]

$$\Delta m = \frac{2\lambda_2}{m}. \quad (2.16)$$

B meson data implies $\lambda_2(\mu = m_b) \approx 0.12 \text{ GeV}$. Using leading log running [?], we get

$$\Delta m = \Delta m_B \left(\frac{m_B}{m_T} \right) \left(\frac{\alpha_s(m_T)}{\alpha_s(m_B)} \right)^{3/(11-2n_f/3)}. \quad (2.17)$$

Once the new particle mass is determined, we can therefore calculate Δm . For example, using $m_t = 170 \text{ GeV}$, $n_f = 5$ and $\alpha_s(m_t)/\alpha_s(m_B) \approx 3.5$ we get

$$\Delta m \approx 1 \text{ MeV}. \quad (2.18)$$

While this is only a rough estimate it serves two purposes. First, we learn that Δm is in the range that is of interest to us. Second, we see that in principle we can get quite an accurate determination of Δm . If needed, higher order corrections can be included.

Next we move to the calculation of Γ_γ . We can use heavy quark symmetry and D^* decay data to get Γ_γ for much heavier mesons. Following [?] and [?] the decay rate can be parameterized as

$$\Gamma_\gamma^a = \frac{\alpha}{3} |\mu^a|^2 |k_\gamma|^3, \quad (2.19)$$

where $a = u, d, s$ is the light quark index, α is the fine structure constant, k_γ is the photon momentum, and μ^a is a coupling constant of dimension -1 . We have basically two unknowns in Eq. (2.19), $|k_\gamma|$ and $|\mu^a|$. For a very heavy quark the photon momentum is given by $|k_\gamma| = \Delta m_T$, a quantity we already discussed, see Eq. (2.17). The calculation of $|\mu^a|$ is more complicated. Both the light and heavy quarks contribute to μ^a , but their contributions scale like $1/m_q$. For the D case, where $1/m_c$ is not very small, the charm contribution is important. In our case,

however, since the top is very heavy, we can neglect its contribution to μ^a . We only need the contributions of the light quarks in order to calculate μ^a .

To calculate μ^a we use the approximate flavor SU(3) symmetry. In the SU(3) symmetry limit μ^a is proportional to one reduced matrix element [?]

$$\mu^a = q_a \beta, \quad (2.20)$$

where q_a is the electric charge of the light quark, and β is the reduced matrix element. When SU(3) breaking effects are included, the simple ratio of 2 : 1 : 1 is not maintained. To get a rough estimate we use here the simple quark model prediction [?]

$$\begin{aligned} \mu_u &= \frac{2}{3}\beta - \frac{g^2}{4\pi} \left(\frac{m_K}{f_K^2} - \frac{m_\pi}{f_\pi^2} \right), \\ \mu_d &= -\frac{1}{3}\beta - \frac{g^2}{4\pi} \frac{m_\pi}{f_\pi^2}, \\ \mu_s &= -\frac{1}{3}\beta - \frac{g^2}{4\pi} \frac{m_K}{f_K^2}, \end{aligned} \quad (2.21)$$

where g is the effective $T^* T \pi$ coupling. While at present our knowledge of the values of β and g is limited, if needed in the future much more precise values can be obtained using the lattice or updating the analysis of [?]. For us it is enough to use rough values for these parameters. We use the following representative values

$$\beta \sim 3 \text{ GeV}^{-1}, \quad g \sim 0.5. \quad (2.22)$$

(The above values are different from those found in [?]. The reason for it is that the data changed. The above values are roughly the best fit values using current data [?].) For $m_t = 170 \text{ GeV}$ and $\Delta m = 1 \text{ MeV}$ we obtain

$$\Gamma_\gamma^u \approx 1.0 \times 10^{-2} \text{ eV}, \quad \Gamma_\gamma^d \approx 2.5 \times 10^{-3} \text{ eV}, \quad \Gamma_\gamma^s \approx 2.5 \times 10^{-3} \text{ eV}. \quad (2.23)$$

We learn that we can expect $\Delta\Gamma$ of order of 10^{-2} eV . This value correspond to lifetimes that are within the problematic region.

We conclude this section with two comments. First we mention that Δm and $\Delta\Gamma$ scale differently as a function of the heavy quark. The leading order scaling is

$$\Delta m \propto m_t^{-1}, \quad \Delta\Gamma \propto m_t^{-3}. \quad (2.24)$$

The strong dependence of y on the heavy quark mass make it such that for very heavy quarks $\Delta\Gamma$ may be very small.

Second we note that $\Delta\Gamma$ is not flavor universal. This is since the width scales like the square of the light quark electric charge. The fact that the width is not flavor universal can help us to get more precise information about the heavy quark lifetime. We know the hadronization flavor ratio, and therefore we have several time scales that control the depolarization. We obtain

$$r = P(\Lambda_t) + \frac{1}{2} \left[\frac{1 - P(\Lambda_t)}{1 + x^2} + \frac{P(T_u)}{1 + y_u} + \frac{P(T_d)}{1 + y_d} + \frac{P(T_s)}{1 + y_s} \right]. \quad (2.25)$$

where $y_a \equiv (\Gamma_a^2/2\Gamma)$ and $P(X)$, the hadronization probability into hadron X , are assumed to be known, see Eq. (2.15). We also used $P(\Lambda_t) + P(T_u) + P(T_d) + P(T_s) = 1$. Eq. (2.25) is an improvement over its simplified version, Eq. (2.13). We see that it involves several time scales and thus a refined way to probe Γ if it happened to be of the order of Γ_γ .

2.4 Discussions and conclusions

We discussed only a top like heavy particle, that is, a color triplet spin half heavy fermion. Our method can be extended to other representation. Clearly, it can work only for particles that are charged under the strong interaction and are not scalars. For such cases, however, it is harder to calculate Δm and $\Delta\Gamma$ since we do not have similar systems that we can use to extrapolate like we did with the b and c quarks. Yet, we do not see a fundamental obstacle to calculate it using models for QCD or on the lattice.

There are several issues that have to be under control before our method can be used:

1. We must know the spin and the $SU(3)_C$ representation of the new particle.
2. We must have a reliable way to calculate its initial polarization.
3. We need a way to measure the polarization when the heavy particle decays.

We do not discuss these issues in detail here. We mention that we would like to know all that independently of our motivation. We do, however, show that in some cases there are ways around some of the above requirements.

If we work within a given model, we can calculate the first two items. That is, once all the model parameters are given, we can check if the apparent measurement of the lifetime using our method agrees with the model prediction.

There is, in principle, a model independent way to avoid the need to know the initial polarization. Consider a situation where we can experimentally sep-

arate events where the top hadronizes into a baryon or a meson. Then, the baryonic events can be used to measure the initial polarization since for such events there is no depolarization effects, and the mesonic event can be used to measure the final polarization.

We did not discuss the possibility of spectator decay $s \rightarrow ue^{-}\bar{\nu}$. This decay introduces a new time scale which could in principle add an additional probe on the lifetime by changing the polarization in the case of the spectator is an s -quark. We did not study this decay in detail, and only comment that it can be relevant for heavy particles where Γ_γ is very small.

To conclude, we show that hadronization can be used to probe lifetimes of particles with intermediate width. The basic idea is that the depolarization time depends on known QCD dynamics. For particles with weak scale masses, the depolarization time happen to be in the region that corresponds to intermediate lifetimes. Therefore, a measurement of the amount of depolarization can be used to determine the lifetime of such a particle.

CHAPTER 3
MATCHING NEUTRINO SECTOR IR OPERATORS TO BSM UV
THEORIES

Based on the 2011 article “Non-Standard Neutrino Interactions at One Loop,”
written in collaboration with Yuval Grossman, Brando Bellazzini, and
published in JHEP **1106**, 104 (2011).

3.1 Introduction

There are many experimental results confirming that neutrinos have masses and oscillate between different flavors [?]. It is plausible that neutrinos acquire small masses from some high scale physics via the see-saw mechanism [?]. If such high energy dynamics are the only source of lepton flavor violation (LFV), neutrino oscillations could remain their only observable effects.¹ It is possible, however, that extra sources of LFV are present at the weak scale. Such LFV sources could induce lepton number violating decays of charged leptons such as $\mu \rightarrow e\gamma$, $\mu \rightarrow eee$ and $\tau \rightarrow \mu\gamma$. Weak scale LFV interactions can also affect neutrino oscillation experiments. For instance, flavor violating Non-Standard Interactions (NSIs) can modify neutrino propagation in matter [?, ?, ?, ?, ?, ?].

NSIs could also affect the production and detection processes generating “wrong flavor” neutrinos [?, ?, ?]. Consider for instance an appearance experiment where a neutrino is produced in association with a muon, and a tau is detected at the detector. The standard interpretation of such a result is that it is due to $\nu_\mu \rightarrow \nu_\tau$ oscillations. This interpretation is correct as long as the produced neutrino is orthogonal to the detected one. However, if there are NSIs that violate the flavor symmetry at the source, the produced neutrino, which we denote by $|\nu_\mu^s\rangle$ is not a simple flavor eigenstate. Analogously, in the presence of detector NSIs, the final state, which we denote as $|\nu_\tau^d\rangle$, is not a simple flavor eigenstate. If these states are not orthogonal, that is,

$$\langle \nu_\mu^s | \nu_\tau^d \rangle \equiv \varepsilon_{\mu\tau} \neq 0, \quad (3.1)$$

tau appearance can occur without oscillation.

¹A remarkable exception arises in the context of supersymmetric theories where such high scale dynamics could leave indelible footprints on the soft terms of the light sparticles via interactions not suppressed by inverse powers of the high scale [?, ?].

In order to describe the effect of NSIs on neutrino oscillation experiments, let us discuss first a simple case with only two generations and a mixing angle $\theta = \pi/4$. Consider also the case when the detector is at a distance L much smaller than one oscillation length,

$$x \equiv \frac{\Delta m^2 L}{4E} \ll 1. \quad (3.2)$$

In this case the oscillation amplitude simply reads $\mathcal{A}_{\text{osc}}(\nu_\mu \rightarrow \nu_\tau) \approx ix$. When NSIs are present, they induce an extra contribution, $\mathcal{A}_{\text{NSI}}(\nu_\mu \rightarrow \nu_\tau) = \varepsilon_{\mu\tau}$. Thus, to leading order in x , the total appearance probability is given by the squared of the sum of amplitudes

$$\mathcal{P}(\nu_\mu \rightarrow \nu_\tau) \approx |\mathcal{A}_{\text{osc}} + \mathcal{A}_{\text{NSI}}|^2 \approx x^2 + |\varepsilon_{\mu\tau}|^2 + 2x \text{Im}(\varepsilon_{\mu\tau}). \quad (3.3)$$

The above simplified result has all the physics in it: the first term is the pure oscillation term, the second one is the x independent term that arises due to the NSIs, and the third term is an interference term. Note that, when $x \gg \varepsilon_{\mu\tau}$, the probability to detect a new physics effect is *enhanced* by the interference term, which is linear in $\varepsilon_{\mu\tau}$, compared to the typical quadratic dependence of lepton flavor violating decays of charged leptons [?]. This fact triggered renewed interest at present neutrino facilities [?, ?, ?, ?, ?]. The typical bounds on production and detection NSIs are about $\varepsilon_{\mu\tau} \sim 10^{-2}$ [?, ?]. Higher sensitivities, of $\varepsilon_{\mu\tau} \lesssim 10^{-3}$ are within the reach of future neutrino experiments [?, ?, ?, ?, ?, ?, ?, ?].

In this paper we study NSIs at the loop level, extending the formalism of [?, ?]. We present a general framework that allows one to extract in a consistent way the physical parameters $\varepsilon_{\alpha\beta}$ (with $\alpha, \beta = 1, 3$) which arise at the loop level either from corrections to the tree level W exchange diagram or from more general corrections, in particular from scalar charged currents. We show how the physical parameter, $\varepsilon_{\alpha\beta}$, can be obtained from the various loop amplitudes

which include vertex corrections, wave function renormalizations, mass corrections as well as box diagrams.

In the case of universal corrections to the W exchange amplitudes, NSIs emerge at one loop because after the Electroweak Symmetry Breaking (EWSB) the kinetic terms and the W couplings are generally not universal in the same basis. Rotating to the mass basis for the charged leptons, the misalignment between vertex and wave functions induce NSIs. We show that the associated $\varepsilon_{\alpha\beta}$ are finite because the $SU(2)_L$ gauge symmetry protects them from possibly divergent contributions.

This paper is organized as follows. In Sec. 3.2, we recall the standard formalism for NSIs. In Sec. 3.3, we extend it to account for loop induced NSIs. In Sec. 3.4, we discuss NSIs at one loop in the R-parity conserving Minimal Supersymmetric Standard Model (MSSM) with generic LFV sources in the soft sector, leaving the details of the calculation to the appendix. Finally, we present our conclusions in Sec. 3.5.

3.2 Notations and formalism

We start by setting our notations to follow Refs. [?, ?]. We first consider only tree level processes and later discuss one loop effects.

Neutrino mass eigenstates are denoted by $|v_i\rangle$, $i = 1, 2, 3$, while $|v_\alpha\rangle$ are the tree level weak interaction partners of the charged lepton mass eigenstates α^- , $\alpha = e, \mu, \tau$. These two bases are related by

$$|v_\alpha\rangle = \sum_i U_{\alpha i} |v_i\rangle. \quad (3.4)$$

where U is the leptonic mixing matrix, the so-called PMNS matrix [?].

We consider experiments where neutrinos are produced at the source in conjunction with incoming negative or outgoing positive charged leptons. Then, the neutrinos travel to the detector where they are detected by producing negative charged leptons. We consider new physics in the production and detection processes assuming that these NSIs have the same Dirac structure as the SM interactions and thus the amplitudes add coherently. We parameterize the new interactions at the source and at the detector by two sets of effective four-fermion couplings,

$$(G_{\text{NP}}^s)_{\alpha\beta}, \quad (G_{\text{NP}}^d)_{\alpha\beta}, \quad (3.5)$$

where α is the charged lepton index and β is the flavor of the neutrino in the weak interaction basis. At tree level, the $SU(2)_L$ gauge symmetry implies that in the SM the four-fermion couplings are proportional to $G_F\delta_{\alpha\beta}$. New interactions, however, allow for non-diagonal and non-universal couplings.

Phenomenological constraints imply that the new interactions are suppressed with respect to the weak interactions. It is thus convenient to define small dimensionless quantities in the following way:

$$\epsilon_{\alpha\beta}^p \equiv \frac{(G_{\text{NP}}^p)_{\alpha\beta}}{\sqrt{|G_F + (G_{\text{NP}}^p)_{\alpha\alpha}|^2 + \sum_{\gamma \neq \alpha} |(G_{\text{NP}}^p)_{\alpha\gamma}|^2}} \quad p = s, d. \quad (3.6)$$

We denote by $|\nu_\alpha^s\rangle$ the neutrino states that is produced at the source, and by $|\nu_\alpha^d\rangle$ the neutrino state that is detected

$$|\nu_\alpha^p\rangle = \frac{G_F\delta_{\alpha\beta} + (G_{\text{NP}}^p)_{\alpha\beta}}{\sqrt{|G_F + (G_{\text{NP}}^p)_{\alpha\alpha}|^2 + \sum_{\gamma \neq \alpha} |(G_{\text{NP}}^p)_{\alpha\gamma}|^2}} |\nu_\beta\rangle \quad p = s, d. \quad (3.7)$$

At the leading order, we have

$$\epsilon_{\alpha\beta}^p = \frac{(G_{\text{NP}}^p)_{\alpha\beta}}{G_F}, \quad |\nu_\alpha^p\rangle = |\nu_\alpha\rangle + \epsilon_{\alpha\beta}^p |\nu_\beta\rangle. \quad (3.8)$$

The expression for the non-orthogonality parameter $\varepsilon_{\alpha\beta}$ at the leading order is given by

$$\varepsilon_{\alpha\beta} \equiv \langle \nu_\alpha^s | \nu_\beta^d \rangle = \begin{cases} 1 + \mathcal{O}(\varepsilon^2) & \alpha = \beta \\ \varepsilon_{\alpha\beta}^{s*} + \varepsilon_{\beta\alpha}^d + \mathcal{O}(\varepsilon^2) & \alpha \neq \beta \end{cases}, \quad (3.9)$$

where by $\mathcal{O}(\varepsilon^2)$ we refer to effects that are quadratic in ε^s or ε^d . Note that in the SM the non-orthogonality parameter vanishes, $\varepsilon_{\alpha\neq\beta} = 0$.

For simplicity, we consider now a two generation model where the production process is associated with a muon and the detection with a tau. We calculate the following expression for the transition probability

$$P_{\mu\tau} = |\langle \nu_\tau^d | \nu_\mu^s(t) \rangle|^2, \quad (3.10)$$

where $\nu_\mu^s(t)$ is the time-evolved state that was purely ν_μ^s at time $t = 0$. Using an explicit parameterization of the neutrino mixing matrix

$$U = \begin{pmatrix} \cos \theta & \sin \theta \\ -\sin \theta & \cos \theta \end{pmatrix} \quad (3.11)$$

and keeping terms up to leading order in ε we get

$$P_{\mu\tau} = \sin^2 x \left\{ \sin^2 2\theta + \mathcal{R}e(\varepsilon_{\tau\mu}^d - \varepsilon_{\mu\tau}^s) \sin 4\theta \right\} + \sin 2x \mathcal{I}m(\varepsilon_{\mu\tau}) \sin 2\theta, \quad (3.12)$$

where

$$\Delta m_{ij}^2 \equiv m_i^2 - m_j^2, \quad x_{ij} \equiv \frac{\Delta_{ij} L}{4E}, \quad x = x_{12}, \quad (3.13)$$

m_i are the neutrino masses, E is the neutrino energy and L is the distance between the source and the detector.

A few remarks are in order regarding Eq. (3.12):

- We keep only terms up to $\mathcal{O}(\varepsilon)$. This is the reason why there is no effect at $x = 0$.

- The different x dependence of the various terms is important as it can be used to distinguish them experimentally.
- The interference term can be very important when $x \gg \varepsilon$.
- The interference term depends on the imaginary part of the NSIs, that is, it requires CP violation.
- NSIs also affect the term proportional to $\sin^2 x$. Yet, within one experiment this change is absorbed into the definition of θ and cannot be distinguished experimentally.
- In many cases the NSIs are closely related to lepton flavor violating charged lepton decays. However, they have a different dependence on ε . Neutrino oscillation experiments are linear in ε (if $x \gg \varepsilon$) while decays like $\tau \rightarrow \mu e^+ e^-$ are quadratic. This makes neutrino oscillation experiments competitive in sensitivity.
- With three generations the result is more complicated and can be found in [?].

Before concluding this section, we remark on the case of heavy neutrinos. For instance, consider the case of k heavy singlet neutrinos. The mixing matrix is $3 \times (3 + k)$ and the 3×3 mixing matrix for the light neutrinos is not unitary anymore. In this case we have [?]

$$\varepsilon_{\alpha\beta} = \sum_h U_{h\alpha} U_{h\beta}^* . \quad (3.14)$$

The point is that using neutrino oscillation experiments we can measure ε , and claim detection of some new physics, but we can not disentangle the underlying mechanism which generates it.

3.3 One loop NSI

In this section, we extend the NSI formalism of Refs. [?, ?] to include one-loop effects. In particular, we consider universal NSIs from correction to the tree level W interaction and non-universal effects due to box diagrams and scalar charged currents.

3.3.1 Correction to the W exchange amplitude

At tree level, gauge invariance guarantees universality of the W interactions. This universality is kept to all orders for an exact symmetry. For a broken symmetry, however, universality is lost beyond tree level. In the following, we show that one-loop effects make the W couplings and the kinetic terms of the fermions non-universal. In particular, we explain why, in general, in the basis where the kinetic term are canonical, the W interactions are not flavor diagonal.

In the following, we neglect neutrino masses since they give subleading effects to the NSIs, as we will discuss later. Similarly, we do not consider other possible non-universal flavor-diagonal NSIs. They can be there but they are assumed to be small and, to leading order, we can just add them to the effect we are considering here.

On general grounds, one-particle irreducible one-loop effects include the self energy diagrams for the charged leptons and the neutrinos, and the corrections to the W vertex as well. These one-loop diagrams modify the kinetic and mass terms for fermions and the W vertex by factors Z_L^ν , $Z_{L,R}^\ell$, and η_m^ℓ defined as fol-

lows:

$$\begin{aligned}
\mathcal{L}_{\text{eff}} = & \bar{\ell}_{jL} (Z_L^\ell)^{ji} i \not{\partial} \ell_{iL} + \bar{\ell}_{jR} (Z_R^\ell)^{ji} i \not{\partial} \ell_{iR} + \bar{\nu}_{jL} (Z_L^\nu)^{ji} i \not{\partial} \nu_{iL} \\
& - \bar{\ell}_{jR} (m_\ell^\circ + \eta_m^\ell)^{ji} \ell_{iL} - \bar{\ell}_{jL} (m_\ell^{\circ\dagger} + \eta_m^{\ell\dagger})^{ji} \ell_{iR} \\
& - \frac{g}{\sqrt{2}} W_\mu^- \bar{\ell}_{jL} \gamma^\mu (Z_L^W)^{ji} \nu_{iL} + \text{H.c.} \quad i, j = 1, 2, 3, \quad (3.15)
\end{aligned}$$

where the symbol “ \circ ” refers to “bare” or unrenormalized mass matrices and Z^a are matrices defined as

$$(Z^a)_{ij} = \delta_{ij} + (\eta^a)_{ij} \quad a = \nu, \ell, W. \quad (3.16)$$

Note that Hermiticity of the effective Lagrangian ensures that $(\eta^{\ell,\nu})^\dagger = \eta^{\ell,\nu}$ while η^W may not be Hermitian. While at tree level $\eta^a = 0$, lepton flavor violating loop corrections introduce non-zero η 's. In general, the off-diagonal elements of η^a are finite, while the diagonal terms diverge. Of course, the physics is finite and we discuss how the divergences cancel below. We define

$$\hat{Z}_L^{\ell,\nu} = L_{\ell,\nu}^\dagger Z_L^{\ell,\nu} L_{\ell,\nu}, \quad \hat{Z}_R^\ell = R_\ell^\dagger Z_R^\ell R_\ell, \quad (3.17)$$

such that $\hat{Z}_{L,R}^a$ are diagonal matrices of positive elements, and L_ℓ and R_ℓ are unitary matrices. We rescale the lepton fields to make their kinetic terms canonical

$$\nu_L \rightarrow L_\nu (\hat{Z}_L^\nu)^{-\frac{1}{2}} \nu_L, \quad \ell_L \rightarrow L_\ell (\hat{Z}_L^\ell)^{-\frac{1}{2}} \ell_L, \quad \ell_R \rightarrow R_\ell (\hat{Z}_R^\ell)^{-\frac{1}{2}} \ell_R. \quad (3.18)$$

where $(\hat{Z}^a)^{-1/2}$ is shorthand for the diagonal matrix of element $(\hat{Z}^a)_{ii}^{-1/2}$. The charged lepton mass terms become

$$\mathcal{L}_{\text{mass}} = -\bar{\ell}_{jR} (\hat{Z}_R^\ell)^{-\frac{1}{2}} R_\ell^\dagger (m_\ell^\circ + \eta_m^\ell) L_\ell (\hat{Z}_L^\ell)^{-\frac{1}{2}} \ell_{iL} + \text{h.c.} \quad (3.19)$$

The mass terms (3.19) can be diagonalized by two independent rotations

$$\ell_L \rightarrow L_m \ell_L, \quad \ell_R \rightarrow R_m \ell_R, \quad (3.20)$$

where L_m and R_m are unitary matrices. We obtain

$$\left[R_m^\dagger (\hat{Z}_L^\ell)^{-\frac{1}{2}} R_\ell^\dagger (m_\ell^\circ + \eta_m^\ell) L_\ell (\hat{Z}_L^\ell)^{-\frac{1}{2}} L_m \right]^{ij} = (m_\ell)_{ij}, \quad (3.21)$$

where m_ℓ is diagonal. After performing the rescaling (3.18) and the field rotation (3.20), the kinetic terms are canonical and the charged lepton mass matrix is diagonal, whereas the interaction terms are not diagonal. For later convenience, we rotate the neutrino fields as $\nu_L \rightarrow L_m \nu_L$, in order to keep them as much aligned as possible with their charged partners. Note that this choice is allowed because when we study NSIs we can neglect neutrino masses. As a result, the W -boson vertices become

$$\mathcal{L}_{int} = -\frac{g_2}{\sqrt{2}} W_\mu^- \bar{\ell}_L \gamma^\mu Z \nu_L - \frac{g_2}{\sqrt{2}} W_\mu^+ \bar{\nu}_L \gamma^\mu Z^\dagger \ell_L, \quad (3.22)$$

where

$$Z = L_m^\dagger (\hat{Z}_L^\ell)^{-\frac{1}{2}} L_\ell^\dagger Z_L^W L_\nu (\hat{Z}_L^\nu)^{-\frac{1}{2}} L_m, \quad (3.23)$$

Let us stress that eq. (3.23) is valid to all orders in perturbation theory. Finally, the relation to the physical parameter $\varepsilon_{\alpha\beta}^W$ can be derived from eq. (3.7) and is given by

$$\varepsilon_{\alpha\beta}^W = \langle \nu_\alpha^s | \nu_\beta^d \rangle = \frac{(ZZ^\dagger)_{\beta\alpha}}{\sqrt{(ZZ^\dagger)_{\alpha\alpha} (ZZ^\dagger)_{\beta\beta}}}. \quad (3.24)$$

This formula has a simple interpretation. $Z_{\alpha\beta} / \sqrt{(ZZ^\dagger)_{\alpha\alpha}}$ is the normalized state produced at the source, while its conjugate is the one detected.

We proceed to find the leading order expressions for $Z_{\alpha\beta}$ and $\varepsilon_{\alpha\beta}^W$. That is, we will work to one loop level. In this case, we can identify the off-diagonal terms of Z with the NSIs at the source and the detector, and therefore we find

$$Z_{\alpha\beta} = \varepsilon_{\alpha\beta}^{s*} = \varepsilon_{\alpha\beta}^{d*}, \quad \alpha \neq \beta. \quad (3.25)$$

For the physical parameters we then get

$$\varepsilon_{\alpha\beta}^W = Z_{\alpha\beta} + Z_{\beta\alpha}^*, \quad \alpha \neq \beta. \quad (3.26)$$

The same result can be obtained directly from eq. (3.24). Note that $ZZ^\dagger = \delta_{\alpha\beta}$ when Z is unitary. When the deviation from unitarity is small, $ZZ^\dagger = 1 + \varepsilon^W$, we recover the previous result. See also eq. (3.33) below.

At one loop, the transformations for the lepton fields of eq. (3.18) read

$$\nu_L \rightarrow \left(1 - \frac{1}{2}\eta_L^\nu\right)\nu_L, \quad \ell_L \rightarrow \left(1 - \frac{1}{2}\eta_L^\ell\right)\ell_L, \quad \ell_R \rightarrow \left(1 - \frac{1}{2}\eta_R^\ell\right)\ell_R. \quad (3.27)$$

Similarly, to one loop accuracy, the transformations of eq. (3.20) read

$$\ell_L \rightarrow (1 + \delta L_m)\ell_L, \quad \ell_R \rightarrow (1 + \delta R_m)\ell_R. \quad (3.28)$$

The unitarity of L_m and R_m implies that

$$\delta L_m^\dagger = -\delta L_m, \quad \delta R_m^\dagger = -\delta R_m. \quad (3.29)$$

In this approximation, Z is given by

$$Z = 1 + \eta_L^W - \frac{\eta_L^\ell + \eta_L^\nu}{2}, \quad (3.30)$$

where η^ν , η^ℓ , and η^W have to be evaluated at one loop accuracy. Eq. (3.30) shows that, at this level, the dependence of Z on L_m drops completely out (its dependence would be reintroduced at two loop). Then we learn that at leading order the non-orthogonality parameter between the source and detector neutrinos is given by (3.26) and reads

$$\varepsilon_{\alpha\beta}^W = \varepsilon_{\alpha\beta}^{s*} + \varepsilon_{\beta\alpha}^d = \left(\eta_L^{W\dagger} + \eta_L^W - \eta_L^\ell - \eta_L^\nu\right)_{\alpha\beta}, \quad (3.31)$$

where we used the fact that η^ℓ and η^ν are Hermitian.

Eqs. (3.23), (3.26), and (3.31) are the main results of this section. A few remarks are in order when inspecting them:

1. For any given model, eqs. (3.23), (3.26) show how to extract the physical NSI effects out of the calculations of the vertex corrections and the self energies encoded in the rotation mass matrices L_ν , L_ℓ and L_m . However, eq. (3.31) demonstrates that, at one loop accuracy, all we need to do is to calculate η^ν , η^ℓ , and η^W , since L_m starts contributing only at two loop.
2. We note that $\epsilon_{\alpha\beta}^W$ is finite. While each of the diagonal terms in η^a may diverge, the combination is finite because of the $SU(2)_L$ gauge symmetry. This can be seen by the fact that the UV properties are insensitive to EWSB. Thus, the divergent part of η^a is real, flavor universal and independent of a . Therefore, the divergent part of $(\eta_L^{W\dagger} + \eta_L^W - \eta_L^\ell - \eta_L^\nu)_{\alpha\alpha}$, as well as its renormalization scale dependence, cancel. In contrast, the flavor off-diagonal elements of η_L^W and $\eta_L^{\nu,\ell}$ are singularly finite and scale independent, as a result of the GIM mechanism. We stress also that when the electroweak symmetry is restored, $v_{EW} \rightarrow 0$, then the finite parts are flavor universal and $\epsilon_{\alpha\beta}^p \rightarrow 0$. Both results are illustrated in a concrete example below where the η^a are explicitly calculated.
3. Considering the CP-conjugated process, we obtain

$$\mathcal{A}_{NSI}^{CP} = \epsilon_{\beta\alpha}^W = \epsilon_{\alpha\beta}^{W*}. \quad (3.32)$$

So, CP is violated when the η^a have non trivial imaginary parts.

4. Eq. (3.31) admits an interpretation in terms of the scattering amplitudes $\mathcal{M}_{\alpha\beta}$. The idea is to think about neutrinos as invisible intermediate states, and sum over all of them in the propagation process from the source to the detector. Considering a source neutrino associated with a charged lepton α and a detection that is done by a charged lepton β , the scattering amplitude

is given by

$$\mathcal{M}_{\alpha\beta} \propto (ZZ^\dagger)_{\beta\alpha} = \delta_{\beta\alpha} + \left(\eta_L^W + \eta_L^{W^\dagger} - \eta_L^\gamma - \eta_L^\ell \right)_{\beta\alpha} = \delta_{\alpha\beta} + \varepsilon_{\beta\alpha}^W. \quad (3.33)$$

where in the second step we expanded in $\eta_L^{\gamma,l,W}$. Thus, we learn that the non-universal part of the amplitude is just $\varepsilon_{\beta\alpha}^W$.

3.3.2 Non-universal effects

So far, we have considered only NSIs induced by the universal corrections to the W vertex and self energy diagrams. These effects are independent of the production or detection processes as long as these processes are mediated by W exchange. We now move to discuss other loop effects that are not universal, that is, that may be different for different production or detection processes.

As mentioned before, the universal effects are $SU(2)$ breaking effects and therefore suppressed like M_W^2/M_{NP}^2 . In the effective field theory language, this would correspond to the effects induced, after the EWSB, by gauge invariant dimension-six operators like $(\bar{L}_L \tau^a \gamma^\mu L_L)(H^\dagger \tau^a D_\mu H)$, where L_L (H) stands for the lepton (Higgs) doublet, τ^a are either the identity or the $SU(2)$ generators and D_μ is the covariant derivative.

It is then clear that contributions arising from dimension six four-fermion operators, also suppressed by M_W^2/M_{NP}^2 , must be consistently included along with the W -penguin contributions. Therefore, for any given New Physics (NP) model we can write the following expression for the physical $\varepsilon_{\alpha\beta}$ parameter

$$\varepsilon_{\alpha\beta} = \varepsilon_{\alpha\beta}^W + \left(\epsilon_{\alpha\beta}^{S^*} \right)^{dim-6} + \left(\epsilon_{\beta\alpha}^d \right)^{dim-6}. \quad (3.34)$$

where $\varepsilon_{\alpha\beta}^W$ has been already defined in eq. (3.31) and we have assumed both matter effects and higher order operators (with $\dim > 6$) to be negligible.

In this work we are interested in NSIs with the same Dirac structure as the SM interactions. The reason is that they maximally exploit the interference between SM and NP amplitudes. In particular, focusing on realistic production and detection processes like $\mu \rightarrow e\nu_e\bar{\nu}_\alpha$ and $P \rightarrow \mu\nu_\alpha$ (with $P = \pi, K$), the relevant dimension six operators are the following

$$\frac{4G_F}{\sqrt{2}} \left(\delta_{\mu\alpha} + (\varepsilon_{\mu\alpha}^s)^{\dim-6} \right) \left(\bar{\nu}_\alpha \gamma^\lambda P_L \mu \right) \left(\bar{e} \gamma_\lambda P_L \nu_e \right), \quad (3.35)$$

$$\frac{4G_F}{\sqrt{2}} \left(\delta_{\mu\alpha} + (\varepsilon_{\mu\alpha}^d)^{\dim-6} \right) \left(\bar{u} \gamma^\lambda P_L d \right) \left(\bar{\mu} \gamma_\lambda P_L \nu_\alpha \right), \quad (3.36)$$

where $(\varepsilon_{\mu\alpha}^{s,d})^{\dim-6}$ stand for the loop-induced corrections.

As we will discuss in the next section, in the context of supersymmetry $\varepsilon_{\mu\alpha}^{\dim-6}$ might be induced either by means of gaugino/sfermion boxes or through the tree level exchange of charged Higgs with loop induced flavor changing couplings $H\ell\nu$.

3.3.3 Matter effects

So far, we have discussed only NSIs induced by the charged currents. However, we would like to emphasize here that there exist also NSIs in matter via neutral currents, even for negligible SM matter effects.

Indeed, starting from the SM neutral current interactions

$$\mathcal{L}_{\text{eff}} = -\frac{g}{2c_W} Z_\mu \bar{\nu}_{jL} \gamma^\mu \left(Z_L^Z \right)^{ji} \nu_{iL} + \text{H.c.} \quad i, j = 1, 2, 3, \quad (3.37)$$

where hereafter $c_W = \cos \theta_W$ and $s_W = \sin \theta_W$, after performing the rescaling (3.18) and the field rotation (3.20), the Z-boson vertex with neutrinos is given by

$$Z = L_m^\dagger (\hat{Z}_L^\nu)^{-\frac{1}{2}} L_\nu^\dagger Z_L^Z L_\nu (\hat{Z}_L^\nu)^{-\frac{1}{2}} L_m, \quad (3.38)$$

where, again, we rotated the neutrino fields as $\nu_L \rightarrow L_m \nu_L$. At one loop accuracy, eq. (3.38) becomes

$$Z = 1 + \eta_L^Z - \eta_L^\nu. \quad (3.39)$$

We stress that also NSIs induced by the Z-penguin are $SU(2)$ breaking effects and all the considerations made for W-penguin induced NSIs apply also here. Therefore, besides Z-penguin effects, we have to include dimension six four-fermion operators. The relevant neutral interactions are

$$\sqrt{2}G_F \left[\varepsilon_{\mu\alpha}^Z (I_{3L}^f - 2Q_f s_W^2) + (\varepsilon_{\mu\alpha}^{m,f})^{dim-6} \right] (\bar{\nu}_\alpha \gamma^\lambda P_L \nu_\mu) (\bar{f} \gamma_\lambda f), \quad (3.40)$$

where f stands for the fermions in the matter. For normal matter, f could be electrons, protons and neutrons $f = e, p, n$, Q_f is the electric charge of f and I_{3L}^f is the third component of weak isospin of the left-chiral projection of f .

Since we can identify $\varepsilon_{\mu\alpha}^Z = Z_{\mu\alpha}$, the total physical parameter in the matter $\varepsilon_{\mu\tau}^{m,f}$ reads

$$\varepsilon_{\mu\tau}^{m,f} = (I_{3L}^f - 2Q_f s_W^2) (\eta_L^Z - \eta_L^\nu)_{\mu\tau} + (\varepsilon_{\mu\tau}^{m,f})^{dim-6}. \quad (3.41)$$

When matter effects are included, the transition probability $P_{\mu\tau}$ of Eq. (3.12) becomes

$$P_{\mu\tau} \simeq x \sin 2\theta \left[x \sin 2\theta - 2L \sum_f A^f \text{Re}(\varepsilon_{\mu\tau}^{m,f}) \right] + x^2 \text{Re}(\varepsilon_{\tau\mu}^d - \varepsilon_{\mu\tau}^s) \sin 4\theta + 2x \text{Im}(\varepsilon_{\mu\tau}) \sin 2\theta, \quad (3.42)$$

where $A^f = \sqrt{2}G_F n_f$ and we have assumed $x \ll 1$ and constant fermion densities n_f .

A close look to Eq. (3.42) shows that the interference term between the SM and non-SM matter effects ($\varepsilon_{\mu\tau}^{m,f}$) depends only on the real part of $\varepsilon_{\mu\tau}^{m,f}$. By contrast, for NSIs at the production or detection processes ($\varepsilon_{\mu\tau}^{s,d}$), the interference term depends only on the imaginary part of the NSIs.

The situation changes when considering the transition probabilities $P_{e\mu}$ and $P_{e\tau}$ which involve the electron neutrino. In these cases, there are interference terms, driven by charged current SM-effects, which are also sensitive to the real parts of $\varepsilon^{s,d}$ [?].

3.3.4 Scalar charged current

Many UV completions of the SM contain an extended Higgs sector, for example, the MSSM. On general grounds, the presence of at least two Higgs doublets leads to a misalignment between the fermion mass matrices and the Yukawa couplings. As a result, Higgs mediated FCNC processes are induced already at tree level resulting in large effects, unless a flavor protection mechanism is at work. Indeed, the Natural Flavor Conservation (NFC) hypothesis was introduced to deal with this flavor problem. However, even if NFC holds at the tree level, this hypothesis is spoiled by quantum corrections [?]. For instance, if NFC arises as a result of a continuous PQ symmetry, the breaking at the quantum level of such a symmetry (as it is required in order to prevent the appearance of a massless Goldstone boson) would reintroduce FCNC effects [?].

This is the case of supersymmetry where the holomorphy of the superpotential implies a type-II structure of the Higgs potential at the tree level. Yet, the presence of a non-vanishing μ -term (such that $\mu H_u H_d$) induces, after SUSY

breaking, non-holomorphic Yukawa couplings for fermions (such as $\bar{Q}_L d_R H_u^\dagger$) [?] and therefore Higgs-mediated flavor violation is unavoidable [?].

Bearing in mind the above considerations, in the following we perform a model independent analysis of NSIs arising from loop-induced scalar charged currents.

The charged Higgs H^\pm couplings with leptons are described by the following effective Lagrangian

$$\mathcal{L}_{\text{eff}} = \bar{\nu}_{jL} (y_\ell^\circ + \eta^H)^{ji} \ell_{iR} H^+ + \text{H.c.} \quad (3.43)$$

where

$$y_\ell^\circ = \frac{g_2}{\sqrt{2}M_W} m_\ell^\circ \tan\beta \quad (3.44)$$

and we recall that “ \circ ” refers to unrenormalized quantities.

The transformations of eqs. (3.18), (3.20) lead to the following effective Lagrangian valid to all orders in perturbation theory

$$\mathcal{L}_{\text{eff}} = \bar{\nu}_{jL} \left[L_m^\dagger (\hat{Z}_L^\nu)^{-\frac{1}{2}} L_\nu^\dagger (y_\ell^\circ + \eta^H) R_\ell (\hat{Z}_R^\ell)^{-\frac{1}{2}} R_m \right]^{ji} \ell_{iR} H^+ + \text{H.c.} . \quad (3.45)$$

In order to find the leading expansion for the above effective couplings, we proceed as follows. We first rescale the lepton fields at one loop level, see eq. (3.18), so that the charged lepton mass terms become

$$\mathcal{L}_{\text{mass}} = -\bar{\ell}_{jR} (m_\ell^\circ + \delta m_\ell)^{ji} \ell_{iL} + \text{h.c.} , \quad (3.46)$$

where

$$\delta m_\ell \equiv \eta_m^\ell - \frac{1}{2} \eta_R^\ell m_\ell^\circ - \frac{1}{2} m_\ell^\circ \eta_L^\ell . \quad (3.47)$$

Then, we make use of the one loop expansions for the matrices L_m and R_m of eq. (3.28) leading to

$$\left[m_\ell^\circ + \delta m_\ell - \delta R_m m_\ell^\circ + m_\ell^\circ \delta L_m \right]^{ji} = m_\ell^{ji} , \quad (3.48)$$

where m_ℓ is diagonal and we have consistently retained only the leading one-loop terms. At this level, the unitarity condition of Eq. (3.29) ensures that $\text{Re}(\delta L_m^{jj}) = \text{Re}(\delta R_m^{jj}) = 0$ and the corrected mass eigenvalues are given by

$$m_{\ell_j} = m_{\ell_j}^\circ + \text{Re}(\delta m_\ell)_{jj} , \quad (3.49)$$

while the condition of reality for the masses implies

$$\text{Im} \delta R^{jj} - \text{Im} \delta L^{jj} = \frac{\text{Im}(\delta m_\ell)_{jj}}{m_{\ell_j}} . \quad (3.50)$$

Finally, δL_m and δR_m are determined by

$$\delta L_m^{ji} = \frac{m_{\ell_j}(\delta m_\ell)^{ji} + (\delta m_\ell^\dagger)^{ji}m_{\ell_i}}{m_{\ell_i}^2 - m_{\ell_j}^2} \quad j \neq i , \quad (3.51)$$

$$\delta R_m^{ji} = \frac{m_{\ell_j}(\delta m_\ell^\dagger)^{ji} + (\delta m_\ell)^{ji}m_{\ell_i}}{m_{\ell_i}^2 - m_{\ell_j}^2} \quad j \neq i , \quad (3.52)$$

where $m_{\ell_i} = (m_\ell)_{ii}$, that is, it is the i th eigenvalue of m_ℓ . We are ready now to expand Eq. (3.45) up to one loop. By making use of the Eqs. (3.47), (3.49), and (3.50), we obtain the following flavor conserving couplings

$$\mathcal{L}_{\text{eff}}^{H^+} = \bar{\nu}_{iL} \left[y_{\ell_i} \left(1 + \frac{1}{2}\eta_L^\ell - \frac{1}{2}\eta_L^\nu - \frac{\eta_m^{\ell\dagger}}{m_{\ell_i}} \right) + \eta^H \right] \ell_{iR} H^+ + \text{H.c.} \quad (3.53)$$

where

$$y_{\ell_i} = \frac{g_2 m_{\ell_i}}{\sqrt{2} M_W} \tan \beta. \quad (3.54)$$

Again, while each term in Eq. (3.53) is in general divergent and renormalization scale dependent, their sum is finite and scale independent.

For the flavor violating charged Higgs couplings, we find the one loop expression

$$\mathcal{L}_{\text{eff}}^{H^+} = \bar{\nu}_{jL} \left[-y_{\ell_i} \delta L_m + y_{\ell_j} \delta R_m - \frac{1}{2} y_{\ell_i} \eta_L^\nu - \frac{1}{2} y_{\ell_j} \eta_R^\ell + \eta^H \right] \ell_{iR} H^+ + \text{H.c.} , \quad (3.55)$$

and each term in eq. (3.55) is finite and scale independent thanks to the GIM mechanism. Notice that, in contrast to the case of NSIs at the W -boson vertex, we are now sensitive to the rotation mass matrices L_m and R_m already at the one loop level. As we will discuss in the next section, within the MSSM the rotations δL_m and δR_m actually provide the dominant effects to the flavor changing couplings.

Let us consider now the case of $j = 3$, that is relevant for a tau neutrino production. In such a case, the one loop expansions for δL_m and δR_m of eqs. (3.51) and (3.52) take the form

$$(\delta R_m)^{3i} \simeq \left[-\frac{\eta_m^{\ell\dagger}}{m_\tau} + \frac{1}{2}\eta_R^\ell - \frac{m_\mu}{m_\tau} \frac{\eta_m^{\ell\dagger}}{m_\tau} + \frac{m_\mu}{m_\tau} \eta_L^\ell \right]^{3i}, \quad (3.56)$$

$$(\delta L_m)^{3i} \simeq \left[-\frac{\eta_m^\ell}{m_\tau} + \frac{1}{2}\eta_L^\ell \right]^{3i}. \quad (3.57)$$

Finally, inserting the above expressions for δL_m and δR_m in eq. (3.55), we find

$$\mathcal{L}_{\text{eff}}^{H^+} = \bar{\nu}_{\tau L} Z_H^{3i} \ell_{iR} H^+ + \text{H.c.}, \quad (3.58)$$

where

$$Z_H^{3i} = \left[\frac{1}{2}y_{\ell_i}\eta_L^\ell - \frac{1}{2}y_{\ell_i}\eta_L^y - y_\tau \frac{\eta_m^{\ell\dagger}}{m_\tau} + \eta^H \right]^{3i}. \quad (3.59)$$

Let us remark that NSI effects driven by charged scalar currents are expected to be particularly relevant for the neutrino production via charged meson decays. In fact, whenever the relevant Yukawa couplings are proportional to the fermion masses, only processes like $P \rightarrow \ell\nu$ (with $P = K, \pi$), which are helicity suppressed in the SM, might receive large contributions. Other production processes like $\mu \rightarrow e\nu\bar{\nu}$ or detection cross-sections are expected not to be significantly affected by such charged scalar currents. As a result, we now have $\epsilon_{\alpha\beta}^s \gg \epsilon_{\alpha\beta}^d$ and therefore $\epsilon_{\mu\tau} \approx \epsilon_{\mu\tau}^{s*}$. This is in contrast to the case with dominant

NSIs at the W-boson vertex where, as we already discussed, it turns out that

$$\epsilon_{\alpha\beta}^s = \epsilon_{\alpha\beta}^d.$$

We can proceed now to establish the relation between $\epsilon_{\mu\tau}$ and Z_H^{32} in the case where the neutrino source is given by the process $\pi \rightarrow \mu\nu$. This decay is mediated by tree level W^\pm and H^\pm exchanges. The relevant effective Lagrangian describing this process is

$$\frac{4G_F}{\sqrt{2}} V_{ud} (\bar{u}\gamma_\mu P_L d) (\bar{\mu}\gamma^\mu P_L \nu_\mu) + V_{ud} \left(\frac{y_d Z_H^{32*}}{m_{H^\pm}^2} \right) (\bar{u} P_R d) (\bar{\mu} P_L \nu_\tau), \quad (3.60)$$

where $P_{R,L} = (1 \pm \gamma_5)/2$ and y_d is the down quark Yukawa coupling. Since the π meson is a pseudoscalar, its decay amplitude can be induced only by the axial-vector part of the W^\pm coupling and the pseudoscalar part of the H^\pm coupling. Then, once we implement the PCAC relations

$$\langle 0 | \bar{u}\gamma_\mu \gamma_5 d | \pi^- \rangle = i f_\pi p_\pi^\mu, \quad \langle 0 | \bar{u}\gamma_5 d | \pi^- \rangle = -i f_\pi \frac{m_\pi^2}{m_d + m_u}, \quad (3.61)$$

we get the amplitudes

$$\mathcal{M}_{\pi \rightarrow \mu \nu_\mu}^W = \frac{G_F}{\sqrt{2}} V_{ud} f_\pi m_\mu \bar{\mu} (1 - \gamma_5) \nu_\mu, \quad (3.62)$$

$$\mathcal{M}_{\pi \rightarrow \mu \nu_\tau}^H = -\frac{V_{ud} f_\pi}{4} \left(\frac{y_d Z_H^{32*}}{m_{H^\pm}^2} \right) \frac{m_\pi^2}{m_d + m_u} \bar{\mu} (1 - \gamma_5) \nu_\tau. \quad (3.63)$$

We observe that the SM amplitude depends on the lepton mass because of the helicity suppression, in contrast to the charged Higgs amplitude which does not suffer from this suppression. Yet, many NP models predict the Yukawa couplings to be proportional to the fermion masses. Effectively then, in such models both the W-boson and charged Higgs amplitudes have the same lepton mass dependence.

Finally, recalling that the produced neutrino state is $|\nu^s\rangle = |\nu_\mu\rangle + \epsilon_{\mu\tau}^s |\nu_\tau\rangle$, we identify

$$\epsilon_{\mu\tau}^\pi \approx (\epsilon_{\mu\tau}^{s*})^\pi = -\frac{\sqrt{2}}{4G_F} \left(\frac{m_\pi^2}{m_d + m_u} \right) \left(\frac{y_d Z_H^{32}}{m_\mu m_{H^\pm}^2} \right). \quad (3.64)$$

In the case of $K \rightarrow \mu\nu$, the relevant parameter $\varepsilon_{\mu\tau}^K$ can be simply obtained from $\varepsilon_{\mu\tau}^\pi$ through the replacement $(m_\pi, y_d, m_d) \rightarrow (m_K, y_s, m_s)$ and we get

$$\frac{\varepsilon_{\mu\tau}^\pi}{\varepsilon_{\mu\tau}^K} \simeq \frac{m_\pi^2}{m_K^2} \frac{m_s + m_u}{m_d + m_u} \frac{y_d}{y_s} \sim \frac{1}{20}. \quad (3.65)$$

It has yet to be seen which process $\pi \rightarrow \mu\nu$ or $K \rightarrow \mu\nu$ may represent the best probe of this scenario when combining the more intense neutrino flux obtainable from $\pi \rightarrow \mu\nu$ with the higher NP sensitivity of $K \rightarrow \mu\nu$.

3.4 One loop NSIs and Supersymmetry

In this section, we apply the model-independent formalism developed in the previous section to the case of the R-parity conserving MSSM with new sources of LFV in the soft sector. We will analyse first loop-induced NSIs from the $V - A$ charged current, passing then to NSIs from the charged scalar current induced by the heavy Higgs sector of the MSSM.

3.4.1 $V - A$ charged current

In the MSSM NSIs may be induced by the $V - A$ charged current through W -penguin as well as box contributions. The former effect arises only after the EWSB and therefore is suppressed by M_W^2/M_{NP}^2 . In particular, within the MSSM, there are three possible sources of $SU(2)$ breaking:

- i) the D -terms,
- ii) the left-right mixing terms, and

iii) the neutralino/chargino mixing terms.

The latter comes from dimension six four-fermion operators and is also suppressed by M_W^2/M_{NP}^2 .

The full analytical calculation relevant for NSIs in the MSSM, upon which our numerical analysis is based on, is reported in the appendix. In the following, instead, we prefer to discuss general properties within an illustrative toy model which is a particular limit of the MSSM that greatly simplifies the calculation but still retains the most relevant features. We use standard MSSM notation (for a review see for example, Ref. [?]) and we consider only the lepton sector.

In our toy model, we decouple the Higgsinos, \tilde{H} , by taking a large μ -parameter and we decouple the Winos, \tilde{W} , by taking their soft mass term, M_2 , to be very large. We also assume left-right mixing between the sleptons to be negligible. Finally, we take the EW vacuum expectation value, v_{EW} , small compared to the soft mass term of the Bino, M_1 , and the soft term for the left-handed sleptons, M_L . That is, we consider a model where

$$\frac{A}{M_L}, \frac{m_\tau \mu \tan \beta}{M_L^2} \ll 1, \quad v_{EW} \ll M_1 \sim M_L \ll \mu \sim M_2. \quad (3.66)$$

where A stands for the trilinear soft terms. In this model there is only one neutralino, the Bino. In practice, the model looks supersymmetric only with respect to $U(1)_Y$. The EWSB can be treated as a perturbation. Note that, in our toy model, only the $SU(2)$ breaking source i) is at work. Later on, we will also discuss the impact on NSIs of sources ii) and iii), which are expected in a more realistic model.



Figure 3.1: 1-loop contributions to the lepton self-energies (left) and to the vertex (right). The virtual particles running in the loop are sleptons and a neutralino.

The relevant interactions are the lepton-Bino-slepton vertex and the slepton-slepton- W vertex, that are given by

$$\mathcal{L}_{NSI} = -\sqrt{2}ig'q_Y\bar{\chi}^0\left(\tilde{\nu}_k^*U_{\tilde{\nu}}^{ki}\nu_i + \tilde{\ell}_k^*U_{\tilde{\ell}}^{ki}\ell_i\right) - \sqrt{2}ig\left(W^\mu\partial_\mu\tilde{\nu}_k\tilde{\ell}_k^*\right) + h.c. \quad (3.67)$$

where $q_Y = -1/2$ is the hypercharge of the left-handed leptons. $U_{\tilde{\nu}}^{ki}$ ($U_{\tilde{\ell}}^{ki}$) is the unitary matrix that diagonalizes the sneutrino (charged slepton) mass matrix. In our model, the soft terms are $SU(2)_L \times U(1)_Y$ symmetric and, since there are no left-right mixings, $U_{\tilde{\nu}} = U_{\tilde{\ell}}$. Thus, from this point on we use $U_{\tilde{\ell}}$ for both terms.

According to Eq. (3.31), all we need to calculate are the loops in Fig. 3.1 and extract η^ν , η^ℓ and η^W . In our calculations we use a naive UV cutoff, that is, we perform the k^2 integral up to Λ^2 . We further introduce an unphysical mass parameter μ to make the arguments of all logarithms dimensionless. Effectively, this is equivalent to introducing a renormalization scale. As a check on our calculation we see that the final physical results, that is, ε , is independent of these two unphysical parameters.

We first calculate the wave function corrections. The only diagrams contributing to η^ν at one loop are through the exchange of the Bino and sneutrinos.

The result is

$$\eta_{ji}^\nu = g'^2 q_Y^2 \sum_k U_{\tilde{\ell}}^{kj*} U_{\tilde{\ell}}^{ki} \mathcal{I}_k^\nu, \quad (3.68)$$

where

$$\mathcal{I}_k^\nu = \frac{1}{16\pi^2} \left\{ \log \frac{\Lambda^2}{\mu^2} + F_k^\nu + \mathcal{O}\left(\frac{1}{\Lambda^2}\right) \right\}, \quad (3.69)$$

$$F_k^\nu = \left[-\log\left(\frac{m_{\tilde{\nu}_k}^2}{\mu^2}\right) + \frac{m_{\chi^0}^4}{(m_{\tilde{\nu}_k}^2 - m_{\chi^0}^2)^2} \log\left(\frac{m_{\tilde{\nu}_k}^2}{m_{\chi^0}^2}\right) - \frac{m_{\tilde{\nu}_k}^2 + m_{\chi^0}^2}{2(m_{\tilde{\nu}_k}^2 - m_{\chi^0}^2)} \right]. \quad (3.70)$$

The calculation of the wave function correction to the left-handed charged leptons η_{ji}^ℓ proceeds in a completely analogous way, the only difference being that now we have sleptons, instead of sneutrinos, running in the loop. Therefore, η_{ji}^ℓ reads

$$\eta_{ji}^\ell = g'^2 q_Y^2 \sum_k U_{\tilde{\ell}}^{kj*} U_{\tilde{\ell}}^{ki} \mathcal{I}_k^\ell, \quad (3.71)$$

where \mathcal{I}_k^ℓ is simply obtained from \mathcal{I}_k^ν by the replacement $m_{\tilde{\nu}_k}^2 \rightarrow m_{\tilde{\ell}_k}^2$.

Next, we calculate the one loop correction to the W vertex, η^W . The result is

$$\eta_{ij}^W = g'^2 q_Y^2 \sum_k U_{\tilde{\ell}}^{kj*} U_{\tilde{\ell}}^{ki} \mathcal{I}_k^W, \quad (3.72)$$

where

$$\mathcal{I}_k^W = \frac{1}{16\pi^2} \left\{ \log \frac{\Lambda^2}{\mu^2} + F_k^W + \mathcal{O}\left(\frac{1}{\Lambda^2}\right) \right\}, \quad (3.73)$$

$$F_k^W = \frac{1}{(m_{\tilde{\nu}_k}^2 - m_{\tilde{\ell}_k}^2)(m_{\tilde{\nu}_k}^2 - m_{\chi^0}^2)(m_{\tilde{\ell}_k}^2 - m_{\chi^0}^2)} \left[m_{\tilde{\nu}_k}^4 (m_{\chi^0}^2 - m_{\tilde{\ell}_k}^2) \log\left(\frac{m_{\tilde{\nu}_k}^2}{\mu^2}\right) + m_{\tilde{\ell}_k}^4 (m_{\tilde{\nu}_k}^2 - m_{\chi^0}^2) \log\left(\frac{m_{\tilde{\ell}_k}^2}{\mu^2}\right) + m_{\chi^0}^4 (m_{\tilde{\ell}_k}^2 - m_{\tilde{\nu}_k}^2) \log\left(\frac{m_{\chi^0}^2}{\mu^2}\right) \right]. \quad (3.74)$$

In order to obtain the final result we use Eq. (3.31) with Eqs. (3.68), (3.71), and (3.72). We get

$$\begin{aligned} \varepsilon &= (\eta^{W\dagger} + \eta^W - \eta^\ell - \eta^\nu) = g'^2 q_Y^2 \sum_k U_{\tilde{\ell}}^{kj*} U_{\tilde{\ell}}^{ki} (2\mathcal{I}_k^W - \mathcal{I}_k^\ell - \mathcal{I}_k^\nu) \\ &= g'^2 q_Y^2 \sum_k U_{\tilde{\ell}}^{kj*} U_{\tilde{\ell}}^{ki} (2F_k^W - F_k^\ell - F_k^\nu), \end{aligned} \quad (3.75)$$

where we neglected $\mathcal{O}(\Lambda^{-2})$ effects.

We are now in a position to check the finiteness of the physical amplitude. Note that η^ν , η^ℓ , and η^W contain a log-divergence. $SU(2)_L$ gauge symmetry constrains the coefficients of these two divergences to be equal to each other. We can see that this is indeed the case by direct inspection. ε in Eq. (3.75) depends only on the functions F^a that are independent of Λ . We can also check that the result is independent of μ , as it should be. For this note that the sum, $2F_k^W - F_k^\ell - F_k^\nu$, is independent of μ . While the above results are automatically achieved by each off-diagonal term contributing to ε , as a result of the GIM-mechanism, their validity for the diagonal components represents a check of the correctness of the calculation.

Another important check is to make sure that in the limit of no EWSB, there is no effect induced by the kinetic term because $SU(2)_L$ gauge symmetry makes it aligned with the W -interaction. When sending $v_{EW} \rightarrow 0$, the charged sleptons become degenerate with the sneutrinos, $m_{l_k}^2 = m_{\tilde{\nu}_k}^2$. In this limit, using (3.75) we learn that the relevant sum is proportional to the identity

$$\varepsilon_{\alpha\beta} \propto \left(\eta_{\alpha\beta}^W + \eta_{\alpha\beta}^{W\dagger} - \eta_{\alpha\beta}^\nu - \eta_{\alpha\beta}^\ell \right) \Big|_{v_{EW}=0} \propto U_{\tilde{\ell}}^\dagger U_{\tilde{\ell}} = \delta_{\alpha\beta} . \quad (3.76)$$

We learn that no flavor changing amplitude is induced thanks to the unitarity of $U_{\tilde{\ell}}$.

The fact that the effect vanishes for $v_{EW} = 0$ can be used to get an approximate formula. We can define the presumably small parameter

$$a_k \equiv \left(\frac{m_{\tilde{\nu}_k}^2 - m_{\tilde{\ell}_k}^2}{m_{\tilde{\ell}_k}^2 + m_{\tilde{\nu}_k}^2} \right), \quad (3.77)$$

that vanishes for $v_{EW} = 0$, and expand in a_k to the leading order

$$\varepsilon_{\alpha\beta} = \left(\eta^W + \eta^{W^\dagger} - \eta^y - \eta^\ell \right)_{\alpha \neq \beta} = \frac{g'^2 q_Y^2}{16\pi^2} U_{\tilde{\ell}}^{k\alpha} U_{\tilde{\ell}}^{k\beta} \sum_k \left[a_k^2 G_k + \mathcal{O}(a_k^3) \right], \quad (3.78)$$

where G_k is a function of SUSY masses which does not vanish in the limit of $a_k \rightarrow 0$. The dominant splitting between left handed sneutrinos and sleptons originates from the D -terms and is flavor universal

$$(m_{\tilde{\nu}_\alpha}^2 - m_{\tilde{\ell}_\alpha}^2) = m_Z^2 \cos^2 \theta_W \cos(2\beta). \quad (3.79)$$

As a result, in this toy model, $\varepsilon_{\mu\tau}$ can be estimated as

$$\varepsilon_{\mu\tau} \sim \frac{\alpha_Y}{4\pi} \cos^4 \theta_W \cos^2(2\beta) \left(\frac{m_Z^2}{\text{Max}[m_{\chi^0}^2, m_{\tilde{\ell}}^2]} \right)^2 \delta_{\mu\tau}^L \lesssim 10^{-6} \delta_{\mu\tau}^L. \quad (3.80)$$

where we have defined the mass-insertion parameters $\delta_{ij}^L = (M_L^2)_{ij} / \sqrt{(M_L^2)_{ii}(M_L^2)_{jj}}$, as usual. Such values are well below the expected experimental resolutions even for $\delta_{\mu\tau}^L \sim 1$.

We discuss now the main differences arising in the cases where the $SU(2)$ breaking sources ii) and iii) are switched on. In the case ii), the leading effect for $\varepsilon_{\mu\tau}$ reads

$$\varepsilon_{\mu\tau} \sim \frac{\alpha_Y m_\tau^2 |A_\tau - \mu \tan \beta|^2}{4\pi m_{\chi^0}^2 m_{\tilde{\ell}}^2} \delta_{\mu\tau}^L, \quad (3.81)$$

where we picked up a double left-right mixing term for the third slepton generation. In principle, $\varepsilon_{\mu\tau}$ could reach values even slightly above 10^{-4} for $m_\tau \mu \tan \beta / m_{\tilde{\ell}}^2 \sim 1$; in practice the constraint from $\tau \rightarrow \mu \gamma$ implies that $\varepsilon_{\mu\tau} < 10^{-5}$.

Finally, in the case iii) we get

$$\varepsilon_{\mu\tau} \sim \frac{\alpha_2}{4\pi} |Z_\pm^{12}|^2 \delta_{\mu\tau}^L, \quad (3.82)$$

where Z_\pm^{12} are the mixing angles of the chargino mass matrix which read

$$Z_+^{12} \approx \frac{v_u M_2 + v_d \mu}{M_2^2 - \mu^2} \quad Z_-^{12} \approx \frac{v_d M_2 + v_u \mu}{M_2^2 - \mu^2}, \quad (3.83)$$

where $\tan\beta = v_u/v_d$. We have explicitly checked that also in this case $\varepsilon_{\mu\tau} < 10^{-5}$ after imposing the constraint from $\tau \rightarrow \mu\gamma$.

We discuss now the box induced NSIs. These effects survive even in the limit where all the $SU(2)$ breaking sources discussed above are negligible. In particular, it turns out that the largest effects arise for light sleptons/Winos and heavy Higgsino/Bino. The latter condition is necessary to suppress $\text{BR}(\tau \rightarrow \mu\gamma)$. As a result, it turns out that

$$\varepsilon_{\mu\tau}^{box} \sim \frac{\alpha_2}{4\pi} \frac{m_Z^2}{\text{Max}[M_2^2, m_{\tilde{\ell}}^2]} \delta_{\mu\tau}^L \lesssim 10^{-3} \delta_{\mu\tau}^L. \quad (3.84)$$

As we will show in the numerical analysis, the box contribution provides the dominant effect to $\varepsilon_{\mu\tau}$ that can reach experimentally interesting levels while being still compatible with the current bound on $\text{BR}(\tau \rightarrow \mu\gamma)$. In fact, in the most favorable situation where $M_2 \sim m_{\tilde{\ell}} \ll \mu \sim M_1$, one can find that

$$|\varepsilon_{\mu\tau}^{box}| \approx 10^{-3} \sqrt{\frac{\text{BR}(\tau \rightarrow \mu\gamma)}{10^{-7}}}, \quad (3.85)$$

as we will confirm numerically.

3.4.2 Scalar charged current

In the MSSM, Higgs mediated LFV effects are generated at the loop level, e.g. see Fig. 3.2. In fact, given a source of non-holomorphic couplings, and LFV among the sleptons, Higgs-mediated LFV is unavoidable [?].

Starting from the model-independent parameterization for the flavor violating couplings of a charged Higgs with leptons, eq. (3.55), we specialize now to a SUSY scenario assuming R-parity conservation to avoid tree level flavor changing effects.

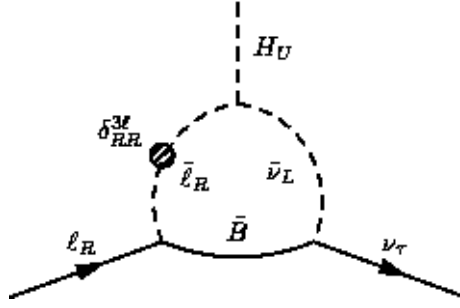


Figure 3.2: A contribution to the effective $\bar{\nu}_\tau \ell_R H^+$ coupling.

Analysing the full expressions of such couplings (reported in the Appendix), we find that the field rotations δL_m and δR_m induce the dominant contributions for the effective Lagrangian of eq. (3.55). In fact, one can show that they are parametrically enhanced by a $\tan\beta$ factor $\delta L_m, \delta R_m \sim [\alpha_2/4\pi] \times \tan\beta$ compared to $\eta^{\ell,\nu} \sim \alpha_2/4\pi$ and $\eta^H \sim y_\ell \times [\alpha_2/4\pi]$.

Since the effects we are going to discuss can be relevant only if $\tan\beta \gg 1$, it turns out that

$$\mathcal{L}_{\text{eff}}^{H^+} \simeq \bar{\nu}_{jL} [y_\ell^\circ - \delta L_m y_\ell^\circ + y_\ell^\circ \delta R_m]^{ji} \ell_{iR} H^+ + \text{H.c.} . \quad (3.86)$$

Retaining only the dominant $\tan\beta$ enhanced contributions in the corrections to the lepton mass matrix, one has that $\delta m_\ell \simeq \eta_m^\ell$ and therefore

$$(\delta m_\ell)_{ij} \simeq m_{\ell_i}^\circ \epsilon t_\beta \delta_{ij} + \epsilon_R t_\beta \delta_R^{ij} m_{\ell_j}^\circ + m_{\ell_i}^\circ \epsilon_L t_\beta \delta_L^{ij}, \quad (3.87)$$

where $\epsilon, \epsilon_{L,R}$ are loop factors of order $\alpha_2/4\pi$ which depend on SUSY mass ratios and $t_\beta \equiv \tan\beta$. Therefore, the rotation matrices can be determined explicitly from eqs. (3.51) and (3.52) and they read

$$\delta L_m^{3i} \simeq \frac{\epsilon_L t_\beta}{(1 + \epsilon t_\beta)} \delta_L^{3i}, \quad \delta R_m^{3i} \simeq \frac{\epsilon_R t_\beta}{(1 + \epsilon t_\beta)} \delta_R^{3i} + 2 \frac{m_{\ell_i}}{m_\tau} \frac{\epsilon_L t_\beta}{(1 + \epsilon t_\beta)} \delta_L^{3i}. \quad (3.88)$$

Finally, in the basis where $\nu_L \rightarrow L_m \nu_L$, the effective Lagrangian for the H^\pm cou-

plings with leptons reads

$$\mathcal{L}_{\text{eff}}^{H^+} \simeq \frac{g_2}{\sqrt{2}M_W} \frac{t_\beta}{1 + \epsilon t_\beta} \bar{\nu}_{jL} \left[m_{\ell_i} \delta^{ji} + m_{\ell_i} t_\beta \Delta_L^{ji} + m_{\ell_j} t_\beta \Delta_R^{ji} \right] \ell_{iR} H^+ + \text{H.c.} \quad (3.89)$$

where we have defined $\Delta_{L(R)}^{ji} \equiv \epsilon_{L(R)} \delta_{L(R)}^{ji} / (1 + \epsilon t_\beta)$.

An inspection of the above effective Lagrangian reveals that: 1) since the Yukawa operator is of dimension four, the quantities $\Delta_{L,R}^{ji}$ depend only on ratios of soft SUSY masses, hence avoiding SUSY decoupling. Yet, the NP effects induced in physical observables will decouple with the charged Higgs mass; 2) the loop induced flavor violating couplings are enhanced by an extra t_β factor compared to the tree level flavor conserving couplings. Therefore the loop suppression can be partially compensated if $\Delta_{L(R)}^{ji} t_\beta \sim 1$; and 3) the flavor violating couplings $H^+ \bar{\ell} \nu_\tau$ (with $\ell = e, \mu$) exhibit a Yukawa enhancement factor m_τ/m_ℓ compared to flavor conserving couplings $H^+ \bar{\ell} \nu_\ell$ when they are induced by Δ_R^{ji} .

Applying the above results to the model-independent parameterization of eq. (3.64), we find

$$\varepsilon_{\mu\tau}^K \approx (\epsilon_{\mu\tau}^{s*})^K = - \left(\frac{m_K^2}{m_{H^\pm}^2} \right) \left(\Delta_L^{32} + \frac{m_\tau}{m_\mu} \Delta_R^{32} \right) \frac{t_\beta^3}{(1 + \epsilon_q t_\beta)(1 + \epsilon t_\beta)}, \quad (3.90)$$

where ϵ_q is a non-holomorphic threshold correction stemming from the quark sector typically of order $\epsilon_q \sim 10^{-2}$.

As seen in eq. (3.65), it turns out that $\varepsilon_{\mu\tau}^\pi / \varepsilon_{\mu\tau}^K \approx 1/20$. We notice that $\varepsilon_{\mu\tau}^\pi$ and $\varepsilon_{\mu\tau}^K$ show an enhanced sensitivity to sources of flavor violation in the right-handed slepton sector thanks to the Yukawa enhancement factor m_τ/m_μ .

In order to quantify the allowed size for $\varepsilon_{\mu\tau}^{K,\pi}$, we have to impose the constraints arising from the charged lepton LFV decays. The most sensitive probe of Higgs mediated effects is generally $\tau \rightarrow \ell_j \eta$ [?] and the corresponding branch-

ing ratio reads

$$\frac{Br(\tau \rightarrow \mu\eta)}{Br(\tau \rightarrow \mu\bar{\nu}_\nu\nu_\tau)} \approx 10^{-2} \left(\frac{|\Delta_{32}^L|^2 + |\Delta_R^{32}|^2}{m_A^4} \right) \frac{t_\beta^6}{|1 + \epsilon_q t_\beta|^2 |1 + \epsilon t_\beta|^2}, \quad (3.91)$$

where m_A is the pseudoscalar mass such that $m_A^2 = m_{H^\pm}^2 - M_W^2$ at tree level. Imposing the experimental constraints from $Br(\tau \rightarrow \mu\eta) \lesssim 10^{-7}$, it turns out that

$$\epsilon_{\mu\tau}^K \lesssim 10^{-2}, \quad \epsilon_{\mu\tau}^\pi \lesssim 5 \times 10^{-4}, \quad (3.92)$$

where the above bounds arise for $|\Delta_{32}^L| \ll |\Delta_R^{32}|$.

Finally, let us mention that Higgs mediated LFV interactions also induce lepton universality breaking effects in $P \rightarrow \ell\nu$ ($\ell = e, \mu$) [?]. However, these effects can only constrain $|\Delta_R^{31}|$ which is unrelated, in general, with the relevant LFV term for NSIs, that is $|\Delta_R^{32}|$.

3.4.3 Numerical analysis

In this section, we provide the predictions for the NSI parameter $\epsilon_{\mu\tau}$ in the framework of the R-parity conserving MSSM with generic LFV soft breaking terms. The allowed values for $\mathcal{I}m(\epsilon_{\mu\tau})$ are obtained after imposing the following constraints: i) the data on flavor physics observables; ii) the mass bounds from direct SUSY searches; iii) the requirement of a neutral lightest SUSY particle; iv) the requirement of correct electroweak symmetry breaking and vacuum stability; and v) the constraints from electroweak precision observables.

Concerning NSI effects driven by the charged Higgs exchange, the most stringent bounds come from the data on LFV and B -physics observables. In particular, the processes $B \rightarrow X_s\gamma$, $B \rightarrow \tau\nu$ and $B \rightarrow D\tau\nu$ are known to be the most

powerful probes of new charged scalar currents. In principle, also the process $B_{s,d} \rightarrow \mu^+ \mu^-$ shows an enhanced sensitivity to extended Higgs sectors. However, since the loop-induced flavor changing coupling $H\bar{b}s(d)$ (with $H = H^0, A^0$) depends on the details of the soft sector, to be conservative, we do not impose here the (model-dependent) constraint from $\text{BR}(B_{s,d} \rightarrow \mu^+ \mu^-)$.

The bounds from $\text{BR}(B \rightarrow X_s \gamma)$ have been obtained employing the SM prediction at the NNLO of Ref. [?], $\text{BR}(B \rightarrow X_s \gamma; E_\gamma > 1.6 \text{ GeV})^{\text{SM}} = (3.15 \pm 0.23) \times 10^{-4}$, combined with the experimental average [?, ?, ?] $\text{BR}(B \rightarrow X_s \gamma; E_\gamma > 1.6 \text{ GeV})^{\text{exp}} = (3.55 \pm 0.24) \times 10^{-4}$. As for the SUSY contributions, we use the calculation of Ref. [?] assuming decoupled gluinos and squarks. For $B \rightarrow \tau \nu$, we use the current world average $\text{BR}(B \rightarrow \tau \nu)_{\text{exp}} = (1.73 \pm 0.35) \times 10^{-4}$ [?], the SM prediction $(1.10 \pm 0.29) \times 10^{-4}$ [?] (see also [?]) and the NP contributions of Ref. [?].

Finally, the NP sensitivity of $B \rightarrow D \tau \nu$ can be better exploited normalizing it to $\text{BR}(B \rightarrow D \tau \nu) / \text{BR}(B \rightarrow D \ell \nu)$ where $\ell = e, \mu$ [?, ?]. We use the world average $(49 \pm 10)\%$ [?] and the theoretical prediction of Ref. [?].

In our numerical analysis we impose all the above constraints at the 2σ C.L..

In Fig. (3.3) on the left, we show the values attained by $|\text{Im}\varepsilon_{\mu\tau}^K|$, see eq. (3.90), in the $\tan\beta - M_{H^\pm}$ plane setting the LFV parameter $|\Delta_R^{32}| = 10^{-3}$ (varying Δ_R^{32} , $|\text{Im}\varepsilon_{\mu\tau}^K|$ would rescale according to $|\Delta_R^{32}|/10^{-3}$). The red, green, blue and yellow regions are excluded by the current bounds on $B \rightarrow X_s \gamma$, $B \rightarrow \tau \nu$, and $B \rightarrow D \tau \nu$ and $\tau \rightarrow \mu \eta$, respectively.

As shown by fig. (3.3), $|\text{Im}\varepsilon_{\mu\tau}^K|$ can vary in the range $(10^{-4}, 10^{-2})$ for $\tan\beta \leq 60$ and $M_{H^\pm} \leq 500 \text{ GeV}$. The corresponding values for $|\text{Im}\varepsilon_{\mu\tau}^\pi|$ can be obtained by

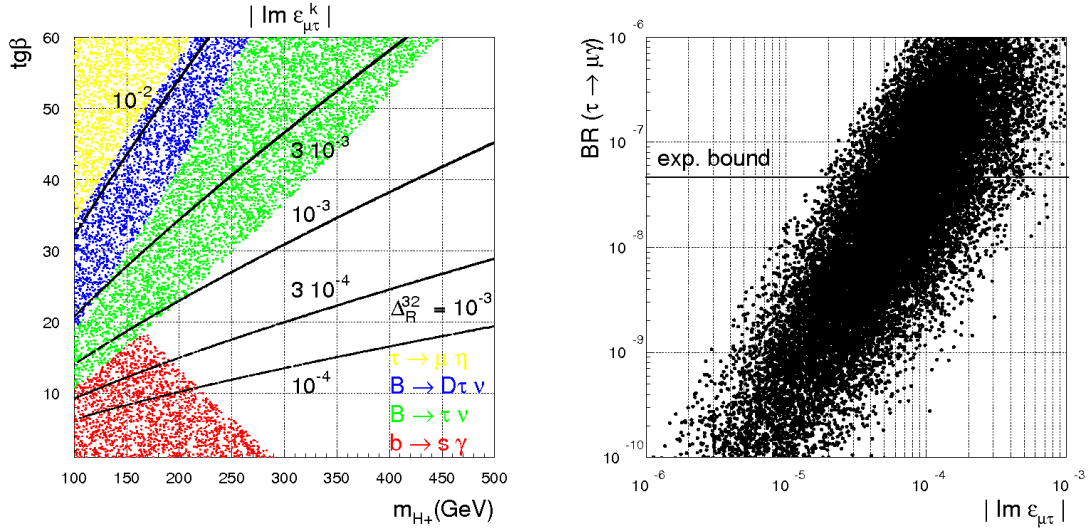


Figure 3.3: Left: NSIs in the process $K \rightarrow \ell \nu$ induced by Higgs mediated effects. Right: NSIs in the process $\mu \rightarrow e \nu \bar{\nu}$ induced by W -penguin and gaugino/slepton boxes. See the text for details.

$$|\text{Im} \epsilon_{\mu\tau}^{\pi}| / |\text{Im} \epsilon_{\mu\tau}^K| \approx 1/20.$$

We now discuss the NSIs as induced by the $V - A$ charged current via the one loop exchange of gauginos/sleptons. As discussed in the above section, the dominant effect to $\text{Im} \epsilon_{\mu\tau}$ arises from the box contributions. In fig. (3.3) on the right, we show the correlation between $\text{BR}(\tau \rightarrow \mu\gamma)$ vs. $|\text{Im} \epsilon_{\mu\tau}|$ in the case where the neutrino source is provided by the muon decay $\mu \rightarrow e \nu_{\tau} \bar{\nu}_e$. We have assumed heavy squarks implying negligible NSIs at the detector level. In this limit also NSIs for the production process $P \rightarrow \mu \nu_{\tau}$ are suppressed. Moreover, as the largest effects for $\text{Im} \epsilon_{\mu\tau}$ are obtained for light sleptons/Winos and heavy Higgsino/Bino (to keep under control $\text{BR}(\tau \rightarrow \mu\gamma)$), we employ the following scan over the SUSY input parameters: $M_2, m_{\tilde{\ell}} \leq 1 \text{ TeV}$, $\mu, M_1 > 500 \text{ GeV}$ and $3 < \tan\beta < 10$.

As shown by fig. (3.3), $|\text{Im}\varepsilon_{\mu\tau}|$ can reach experimentally interesting values $|\text{Im}\varepsilon_{\mu\tau}| \lesssim 3 - 4 \times 10^{-4}$ and this would unambiguously imply a lower bound for $\text{BR}(\tau \rightarrow \mu\gamma)$ quite close to the current bound.

3.5 Discussion and conclusion

The idea that neutrino oscillations can probe NSIs is very attractive. In theory such experiments are sensitive to any form of new physics that makes the produced and detected neutrinos non-orthogonal. Such non-orthogonality, parameterized by $\varepsilon_{\alpha\beta}$, may come from new tree level interactions, new heavy neutrinos, or one loop effects that modify the couplings of the W boson to the leptons.

In this work we presented a general framework that allows one to extract in a consistent way the physical ε arising at the loop level either from the $V - A$ or scalar charged currents. We show how ε can be obtained from the various loop amplitudes which include vertex corrections, wave function renormalizations, mass corrections as well as box diagrams.

As an illustrative example, we discussed NSIs in the R-parity conserving MSSM with new LFV sources in the soft sector.

We argued that, in general, the size of one-loop NSIs is quite small, $\varepsilon \approx O(10^{-3})$. To be observed, such small numbers require very precise measurements of the neutrino appearance probability as a function of L/E . We hope that such measurements will be possible in the next generation of neutrino oscillation experiments.

APPENDIX A
DETAILED FOR LIFETIMES VIA SPIN INFORMATION CALCULATION

A.1 Calculation of spin information being lost through mixing

A.1.1 Assumptions

For the following we assume creating a top meson at $t = 0$ as an incoherent mix of a spin up and down spectator: $T^*: (1/\sqrt{2})(|t:\uparrow, u:\downarrow\rangle + e^{i\phi}|t:\uparrow, u:\uparrow\rangle)$ For the purpose of this calculation we will call the spectator u .

We are assuming we know that t is a spin $\frac{1}{2}$ quark (fundamental representation of QCD) and that the spectator is also a spin $\frac{1}{2}$ quark (fundamental representation of QCD). This assumption is obvious when dealing with the t quark, but for new physics this needs to be determined first.

The t quark decays chirally and we know the chirality of the decay, i.e. we know the numerical difference between the left chirality vertex and the right chirality vertex. (If we don't know that then we face a problem that a semi-chiral fast decay, $\Delta m \ll \Gamma$, will look like a fully chiral slow decay).

We can detect what t decays to. For example, a fermion can decay to a fermion and scalar, or to fermion and vector. (If all we have is jets and the new particle can decay to both gluon and quark, or to quark and squark we may not be able to tag the difference at each decay).

We assume the decay rate of the T and T^* is the same. For a top like particle this is a good assumption to make, because the decay is with weak interactions and only involves the heavy quark.

A.1.2 spin information lost in mixing and vector meson decay

First, to see how the states mix we need to write the top meson mixture in the mass eigenstates.

$$\frac{1}{\sqrt{2}} (|t : \uparrow, u : \downarrow\rangle + |t : \uparrow, u : \uparrow\rangle) = \frac{1}{2} |s = 0, m_s = 0\rangle + \frac{1}{2} (|s = 1, m_s = 0\rangle + \sqrt{2} |s = 1, m_s = 1\rangle) \quad (\text{A.1})$$

Here the scalar top meson is denoted as $T(t = 0) = |s = 0; m_s = 0\rangle$ and the vector top meson spin eigenstates as $T^*(t = 0) = (1/2) (|s = 1, m_s = 0\rangle + \sqrt{2} |s = 1, m_s = 1\rangle)$.

An eigenstate of the Hamiltonian evolves as $|T\rangle = \exp(-iHt) |T(t = 0)\rangle$, thus the time evolved state can be written as follows:

$$\begin{aligned} |T\rangle &= \frac{1}{2} e^{-im_T t - \frac{\Gamma(T \rightarrow \text{final}) - \Gamma(T^* \rightarrow T)}{2} t} |s = 0; m_s = 0\rangle \\ &+ \frac{1}{2} e^{-im_{T^*} t - \frac{\Gamma(T^* \rightarrow \text{final}) + \Gamma(T^* \rightarrow T)}{2} t} (|s = 1, m_s = 0\rangle + \sqrt{2} |s = 1, m_s = 1\rangle) \end{aligned} \quad (\text{A.2})$$

Here we plugged the decay, $T^* \rightarrow T + \gamma$, and the weak decay of the t quark into the Hamiltonian as $\Gamma(T^* \rightarrow T)$ and $\Gamma(T \rightarrow \text{final})$. Therefore, this calculation will include spin information loss through both mixing and T^* decay.

The total phase would not show up in the calculation and can be neglected:

$$\begin{aligned} |T\rangle &\rightarrow e^{-im_{T^*} t} \left(\frac{1}{2} e^{i\Delta m_{T^*} t - \frac{\Gamma_T - \Gamma_{T^* \rightarrow T}}{2} t} |s = 0; m_s = 0\rangle \right. \\ &\left. + e^{-\frac{\Gamma_{T^*} + \Gamma_{T^* \rightarrow T}}{2} t} \left(\frac{1}{2} |s = 1, m_s = 0\rangle + \frac{1}{\sqrt{2}} |s = 1, m_s = 1\rangle \right) \right) \end{aligned} \quad (\text{A.3})$$

Now that we know the evolution of the states we need to go back to the top spin

states:

$$\begin{aligned}
|T\rangle = & \frac{1}{\sqrt{2}} \left[\frac{1}{2} |t : \uparrow, u : \downarrow\rangle \left(e^{-\frac{\Gamma_{T^*} + \Gamma_{T^* \rightarrow T} t}{2}} + e^{i\Delta m_{T^*} t} e^{-\frac{\Gamma_T - \Gamma_{T^* \rightarrow T} t}{2}} \right) \right. \\
& + \frac{1}{2} |t : \downarrow, u : \uparrow\rangle \left(e^{-\frac{\Gamma_{T^*} + \Gamma_{T^* \rightarrow T} t}{2}} - e^{i\Delta m_{T^*} t} e^{-\frac{\Gamma_T - \Gamma_{T^* \rightarrow T} t}{2}} \right) \\
& \left. + e^{-\frac{\Gamma_{T^*} + \Gamma_{T^* \rightarrow T} t}{2}} |t : \uparrow, u : \uparrow\rangle \right] \quad (\text{A.4})
\end{aligned}$$

Then, the spin expectation value, s_z (using $\hbar = 1$) assuming the top is created with its helicity in the z direction:

$$\begin{aligned}
\frac{1}{2} \sigma_z^{\text{Of the top spin space}} |T\rangle = & \frac{1}{\sqrt{2}} \frac{1}{2} |t : \uparrow, u : \downarrow\rangle \left(e^{-\frac{\Gamma_{T^*} + \Gamma_{T^* \rightarrow T} t}{2}} + e^{i\Delta m_{T^*} t} e^{-\frac{\Gamma_T - \Gamma_{T^* \rightarrow T} t}{2}} \right) \\
& - \frac{1}{\sqrt{2}} \frac{1}{2} |t : \downarrow, u : \uparrow\rangle \left(e^{-\frac{\Gamma_{T^*} + \Gamma_{T^* \rightarrow T} t}{2}} - e^{i\Delta m_{T^*} t} e^{-\frac{\Gamma_T - \Gamma_{T^* \rightarrow T} t}{2}} \right) \\
& + \frac{1}{2} e^{-\frac{\Gamma_{T^*} + \Gamma_{T^* \rightarrow T} t}{2}} |t : \uparrow, u : \uparrow\rangle \quad (\text{A.5})
\end{aligned}$$

$$\langle s_z \rangle = \frac{e^{-\Gamma t}}{2} \left(\frac{1}{2} \cos(\Delta m_{T^*} t) + \frac{1}{2} e^{-(\frac{\Delta\Gamma}{2} + \Gamma_{T^* \rightarrow T}) t} \right) \quad (\text{A.6})$$

Finally, we can calculate the ratio, r , between having a spin information loss effect and the result assuming no effect. In this calculation we will denote $\langle s_z \rangle$ as the result above and $\langle s_z \rangle_0$ as the expectation value with no spin information loss. We also denote $x = \frac{\Gamma}{\Delta m_{T^*}}$, $y = \frac{\Gamma_\gamma}{\Gamma}$:

$$\begin{aligned}
\int \langle s_z \rangle_0 dt &= \int_0^\infty e^{-\Gamma t} dt = \frac{1}{\Gamma} \\
\int \langle s_z \rangle dt &= \int_0^\infty e^{-\Gamma t} \left(\frac{1}{2} \cos(\Delta m_{T^*} t) + \frac{1}{2} e^{-\Gamma_{T^* \rightarrow T} t} \right) dt \\
&= \frac{1}{2} \frac{\Gamma}{\Delta m_{T^*}^2 + \Gamma^2} + \frac{1}{2} \frac{1}{\Gamma + \Gamma_\gamma} \\
r = \frac{\int \langle s_z \rangle dt}{\int \langle s_z \rangle_0 dt} &= \frac{1}{2} \left(\frac{1}{1 + (\Delta m_{T^*} / \Gamma)^2} + \frac{1}{1 + \Gamma_\gamma / \Gamma} \right) \\
&= \frac{1}{2} \left(\frac{1}{1 + x^2} + \frac{1}{1 + y} \right) \quad (\text{A.7})
\end{aligned}$$

This method for lifetime determination will be useful for $\Gamma \lesssim 1$ GeV. Therefore, if the decline in spin information happens when x is order one then we need

$\Delta m_T \lesssim 1 \text{ GeV}$. For the case of regular mesons (with a heavy quark) we start the search for new physics with mesons heavier than the B meson. For the B meson we know $\Delta m_B = 45.78(35) \text{ MeV}$. As we will discuss later in this this appendix the mass splitting would only get smaller as the heavy quark gets heavier (as you may expect from an analogy to the hyperfine splitting). Thus, the mass splitting would remain relevant for heavy quarks throughout the weak scale.

A.2 Spin information in the top quark decay

Let us consider a decay with no mixing of a fermion created with its helicity in the z direction into a fermion and a scalar.

$$\sum_{final} |\mathcal{M}|^2 = g^2 m_t E_{fermion} (1 \mp s_z \cos \theta) \quad (\text{A.8})$$

$$\Gamma = \int \frac{d\Gamma}{d\Omega} d\Omega = \frac{1}{8\pi} \frac{E_{fermion}^2}{m_t} g^2 \quad (\text{A.9})$$

$$\frac{d\Gamma}{d\Omega}|_{CM} = \frac{\Gamma}{4\pi} (1 \mp s_z \cos \theta) \quad (\text{A.10})$$

In this section the upper sign refer to P_L and the lower to P_R .

The other option is the decay of a fermion into a fermion and a vector. This case would just involve switching the angular dependance of the left and right vertices:

$$\frac{d\Gamma}{d\Omega}|_{CM} = \frac{\Gamma}{4\pi} (1 \pm s_z \cos \theta) \quad (\text{A.11})$$

For this calculation it's easy to see that a decay into a massive vector, $m_t \sim m_W$, would involve both tangential and longitudinal degrees of freedom and thus the spin information would be washed away.

We are interested with the angular distribution of the decay, so we denote $\rho(t) = \Gamma \exp(-\Gamma t)$ as the distribution function of the decay.

$$\begin{aligned}
P(\Omega) &= \int_0^\infty \left(\rho(t) \frac{d\Gamma}{d\Omega} / \Gamma \right) dt \\
&= \frac{1}{4\pi} \left(\int_0^\infty \Gamma e^{-\Gamma t} dt + \Gamma \int_0^\infty \langle s_z \rangle (\mp \cos \theta) dt \right) \\
&= \frac{1}{4\pi} \left(1 + r\Gamma \int \langle s_z \rangle_0 (\mp \cos \theta) dt \right) \\
&= \frac{1}{4\pi} (1 \mp r \cos \theta)
\end{aligned} \tag{A.12}$$

thus we arrive at the main result

$$P(\Omega) = \frac{1}{4\pi} \left(1 \mp \frac{1}{2} \left(\frac{1}{1+x^2} + \frac{1}{1+y} \right) \cos \theta \right) \tag{A.13}$$

APPENDIX B
DETAILS FOR MATCHING UV BSM THEORIES WITH IR NEUTRINO
SECTOR OPERATORS

B.1 Self-energies and vertex correction in the MSSM

In the following, we provide the full analytical expressions for the self-energies and vertex corrections relevant for NSIs in the R-parity conserving MSSM. For the Feynman rules, we closely follow the notation of Ref. [?].

The lepton self-energies read

$$-(4\pi)^2 (\eta_{VL}^v)^{IJ} = L_{vLC}^{lki} L_{vLC}^{Jki*} B_1(m_{L_k}, m_{C_i}) + L_{v\tilde{\nu}N}^{lki} L_{v\tilde{\nu}N}^{Jki*} B_1(m_{\tilde{\nu}_k}, m_{N_i}) \quad (\text{B.1})$$

$$-(4\pi)^2 (\eta_{VL}^\ell)^{IJ} = L_{eLN}^{lki} L_{eLN}^{Jki*} B_1(m_{L_k}, m_{N_i}) + L_{e\tilde{\nu}C}^{lki} L_{e\tilde{\nu}C}^{Jki*} B_1(m_{\tilde{\nu}_k}, m_{C_i}) \quad (\text{B.2})$$

$$-(4\pi)^2 (\eta_{VR}^\ell)^{IJ} = R_{eLN}^{lki} R_{eLN}^{Jki*} B_1(m_{L_k}, m_{N_i}) + R_{e\tilde{\nu}C}^{lki} R_{e\tilde{\nu}C}^{Jki*} B_1(m_{\tilde{\nu}_k}, m_{C_i}) \quad (\text{B.3})$$

$$(4\pi)^2 (\eta_{mL}^\ell)^{IJ} = -L_{eLN}^{lki} R_{eLN}^{Jki*} B_0(m_{L_k}, m_{N_i}) - L_{e\tilde{\nu}C}^{lki} R_{e\tilde{\nu}C}^{Jki*} B_0(m_{\tilde{\nu}_k}, m_{C_i}). \quad (\text{B.4})$$

The vertex corrections relevant for $W\ell\nu$ are

$$\begin{aligned} (4\pi)^2 (\eta^W)^{IJ} = & \frac{1}{2} L_{v\tilde{\nu}N}^{Jkj*} L_{eLN}^{Iij} Z_v^{Lk*} Z_L^{Li*} \left[B_0(m_{L_i}, m_{\tilde{\nu}_k}) + \frac{1}{2} + m_{N_j}^2 C_0(m_{N_j}, m_{L_i}, m_{\tilde{\nu}_k}) \right] + \\ & + L_{vLC}^{Jki*} L_{eLN}^{lki} \left[\sqrt{2} L_{wCN}^{ji} m_{C_i} m_{N_j} C_0(m_{L_k}, m_{C_i}, m_{N_j}) + \right. \\ & \left. - \frac{1}{\sqrt{2}} R_{wCN}^{ji} \left(B_0(m_{C_i}, m_{N_j}) - \frac{1}{2} + m_{L_k}^2 C_0(m_{L_k}, m_{C_i}, m_{N_j}) \right) \right] \\ & + L_{v\tilde{\nu}N}^{Jkj*} L_{e\tilde{\nu}C}^{lki} \left[-\sqrt{2} R_{wCN}^{ji} m_{C_i} m_{N_j} C_0(m_{\tilde{\nu}_k}, m_{C_i}, m_{N_j}) + \right. \\ & \left. + \frac{1}{\sqrt{2}} L_{wCN}^{ji} \left(B_0(m_{C_i}, m_{N_j}) - \frac{1}{2} + m_{\tilde{\nu}_k}^2 C_0(m_{\tilde{\nu}_k}, m_{C_i}, m_{N_j}) \right) \right]. \quad (\text{B.5}) \end{aligned}$$

The vertex corrections relevant for $H\ell\nu$ are

$$\begin{aligned} (4\pi)^2 (\eta^H)^{IJ} = & -V_{\tilde{\nu}LH}^{ml} L_{v\tilde{\nu}N}^{Jmn*} R_{eLN}^{lm} m_{N_n} C_0(m_{N_n}, m_{\tilde{\nu}_m}, m_{L_l}) \\ & + L_{vLC}^{Jnm*} R_{eLN}^{lnl} \left[L_{NCH}^{lm} C_2(m_{L_n}^2, m_{C_m}^2, m_{N_l}^2) \right. \\ & \quad \left. - R_{NCH}^{lm} m_{C_m} m_{N_l} C_0(m_{L_n}^2, m_{C_m}^2, m_{N_l}^2) \right] \\ & + L_{v\tilde{\nu}N}^{Jnl*} R_{e\tilde{\nu}C}^{lnm} \left[L_{NCH}^{lm} C_2(m_{\tilde{\nu}_n}^2, m_{N_l}^2, m_{C_m}^2) \right. \\ & \quad \left. - R_{NCH}^{lm} m_{N_l} m_{C_m} C_0(m_{\tilde{\nu}_n}^2, m_{N_l}^2, m_{C_m}^2) \right]. \quad (\text{B.6}) \end{aligned}$$

The gaugino/slepton box diagrams relevant for the process $\mu \rightarrow e\nu_\tau\bar{\nu}_e$ read

$$\begin{aligned}
-(4\pi)^2 \epsilon_{IJ}^{\text{box}} &= L_{\ell LN}^{Ikj} L_{\nu LC}^{Jki*} L_{\nu LC}^{eli} L_{\ell LN}^{elj*} D_2(m_{L_k}, m_{L_l}, m_{C_i}, m_{N_j}) \\
&+ L_{\ell\bar{\nu}C}^{IKi} L_{\nu\bar{\nu}N}^{JKj*} L_{\nu\bar{\nu}N}^{eLj} L_{\ell\bar{\nu}C}^{eLi*} D_2(m_{\bar{\nu}_K}, m_{\bar{\nu}_L}, m_{C_i}, m_{N_j}) \\
&+ \frac{1}{2} L_{\ell LN}^{Ikj} L_{\nu\bar{\nu}N}^{eKj} L_{\nu LC}^{Jki*} L_{\ell\bar{\nu}C}^{eKi*} m_{C_i} m_{N_j} D_0(m_{L_k}, m_{\bar{\nu}_K}, m_{C_i}, m_{N_j}) \\
&+ \frac{1}{2} L_{\ell\bar{\nu}C}^{IKi} L_{\nu LC}^{eki} L_{\nu\bar{\nu}N}^{JKj*} L_{\ell LN}^{ekj*} m_{C_i} m_{N_j} D_0(m_{L_k}, m_{\bar{\nu}_K}, m_{C_i}, m_{N_j}). \quad (\text{B.7})
\end{aligned}$$

The box diagrams generated by the gaugino/slepton(squark) exchange contributing to the production process $P \rightarrow \mu\nu_\alpha$ ($P = \pi, K$) and to the detection process read

$$\begin{aligned}
-(4\pi)^2 \epsilon_{IJ}^{\text{box}} &= L_{\ell LN}^{Jkj*} L_{\nu LC}^{Iki} L_{uDC}^{dli*} L_{dDN}^{dlj} D_2(m_{\bar{d}_k}, m_{\bar{d}_l}, m_{C_i}, m_{N_j}) \\
&+ L_{\ell\bar{\nu}C}^{JKi*} L_{\nu\bar{\nu}N}^{IKj} L_{uUN}^{dLj*} L_{dUC}^{dLi} D_2(m_{\bar{\nu}_K}, m_{\bar{u}_L}, m_{C_i}, m_{N_j}) \\
&+ \frac{1}{2} L_{\ell LN}^{Jkj*} L_{uUN}^{dKj*} L_{\nu LC}^{Iki} L_{dUC}^{dKi} m_{C_i} m_{N_j} D_0(m_{L_k}, m_{\bar{u}_K}, m_{C_i}, m_{N_j}) \\
&+ \frac{1}{2} L_{\ell\bar{\nu}C}^{JKi*} L_{uDC}^{dki*} L_{\nu\bar{\nu}N}^{IKj} L_{dDN}^{dkj} m_{C_i} m_{N_j} D_0(m_{\bar{d}_k}, m_{\bar{\nu}_K}, m_{C_i}, m_{N_j}). \quad (\text{B.8})
\end{aligned}$$

The expressions for the loop functions appearing in the above amplitudes read

$$B_0(m_1, m_2) = \frac{1}{\varepsilon} + 1 - \frac{1}{m_1^2 - m_2^2} \left[m_1^2 \log \frac{m_1^2}{\mu^2} - m_2^2 \log \frac{m_2^2}{\mu^2} \right], \quad (\text{B.9})$$

$$B_1(m_1, m_2) = -\frac{1}{2} \left[\frac{1}{\varepsilon} + 1 - \log \frac{m_2^2}{\mu^2} + \left(\frac{m_1^2}{m_1^2 - m_2^2} \right)^2 \log \frac{m_2^2}{m_1^2} + \frac{1}{2} \frac{m_1^2 + m_2^2}{m_1^2 - m_2^2} \right], \quad (\text{B.10})$$

$$C_0(m_1, m_2, m_3) = \frac{1}{m_2^2 - m_3^2} \left[\frac{m_2^2}{m_1^2 - m_2^2} \log \frac{m_2^2}{m_1^2} - \frac{m_3^2}{m_1^2 - m_3^2} \log \frac{m_3^2}{m_1^2} \right], \quad (\text{B.11})$$

$$C_2(m_1, m_2, m_3) = \frac{1}{\varepsilon} + 1 + \log \frac{m_1^2}{\mu^2} + \frac{m_1^4 \log m_2^2/m_1^2}{(m_1^2 - m_2^2)(m_3^2 - m_2^2)} + \frac{m_3^4 \log m_3^2/m_1^2}{(m_1^2 - m_3^2)(m_2^2 - m_3^2)} \quad (\text{B.12})$$

$$\begin{aligned}
D_0(m_1, m_2, m_3, m_4) &= \frac{m_1^2 \log m_1^2}{(m_4^2 - m_1^2)(m_3^2 - m_1^2)(m_2^2 - m_1^2)} \\
&+ \{1 \leftrightarrow 2\} + \{1 \leftrightarrow 3\} + \{1 \leftrightarrow 4\}, \quad (\text{B.13})
\end{aligned}$$

$$\begin{aligned}
D_2(m_1, m_2, m_3, m_4) &= \frac{1}{4} \frac{m_1^4 \log m_1^2}{(m_4^2 - m_1^2)(m_3^2 - m_1^2)(m_2^2 - m_1^2)} \\
&+ \{1 \leftrightarrow 2\} + \{1 \leftrightarrow 3\} + \{1 \leftrightarrow 4\}. \quad (\text{B.14})
\end{aligned}$$

B.2 How self energy and vertex correction enter the theory

Starting for a standard model Lagrangian,

$$\mathcal{L}_{SM} = \bar{L}_i (i \not{\partial} - g \not{W}) L_i \quad (\text{B.15})$$

We will find loop correction to all the terms to some loop level. Then we will be left with the following form,

$$\mathcal{L}_{1\text{-loop NP}} = Z_{ji}^\ell \bar{\ell}_j i \not{\partial} \ell_i + Z_{ji}^\nu \bar{\nu}_j i \not{\partial} \nu_i - Z_{ji}^W \frac{g}{\sqrt{2}} \bar{\nu}_j \not{W}^+ \ell_i + h.c. + \dots \quad (\text{B.16})$$

$$-\bar{\ell}_j M_{ji} \ell_i \quad (\text{B.17})$$

$$Z_{ji} = \delta_{ji}^{(\text{SM})} + \epsilon_{ji}^{(\text{NP})} \quad (\text{B.18})$$

Here we denote $Z_{ji} = \delta_{ji}^{(\text{SM})} + \epsilon_{ji}^{(\text{NP})}$. So it contains the standard model diagonal term and the new physics (off diagonal) contribution.

Now to get to canonical fields with canonical kinetic terms we need to do some field redefinition. This is a part of the calculation which is easy to neglect but without which we will get the wrong result. For example, as was discussed in the thesis above, if the electroweak theory was not broken then we will have alignment between the kinetic terms and the interaction terms and there would be no effect.

We rotate to diagonal kinetic terms, defining the following R^ℓ as the rotation matrix for the leptons. We find, $R^\ell Z_{ji}^\ell R^{\dagger\ell} = Z_{diag}^\ell$, and $R^\ell \ell_i = \ell_{diag}$. We are left with:

$$\begin{aligned} \bar{\ell}_j Z_{ji}^\ell \ell_i &= \bar{\ell} R^{\dagger\ell} R^\ell Z^\ell R^{\dagger\ell} R^\ell \ell \\ &= \bar{\ell}_{diag} Z_{diag}^\ell \ell_{diag} \end{aligned} \quad (\text{B.19})$$

Now to make the field canonical we note:

$$\delta_{ij} = \frac{1}{\sqrt{Z_{diag}}} Z_{diag}^\ell \frac{1}{\sqrt{Z_{diag}}} \quad (\text{B.20})$$

$$\ell_{can} = \sqrt{z_{diag}} R^\ell \ell_i = \sqrt{z_{diag}} \ell_{diag} \quad (\text{B.21})$$

Now that we have canonical kinetic terms to get to the charged lepton mass basis we need to diagonalize the lepton mass. After making the fields canonical we were left with the following,

$$M_{ji} \rightarrow \frac{1}{\sqrt{Z_{diag}}} R^\ell M_{ji} R^{\dagger\ell} \frac{1}{\sqrt{Z_{diag}}}. \quad (\text{B.22})$$

Thus to diagonalize let's define a rotation matrix R_m .

$$\begin{aligned} \bar{\ell}_{can} \frac{1}{\sqrt{Z_{diag}}} R^\ell M_{ji} R^{\dagger\ell} \frac{1}{\sqrt{Z_{diag}}} \ell_{can} &= \bar{\ell}_{can} R_m^\dagger R_m \frac{1}{\sqrt{Z_{diag}}} R^\ell M_{ji} R^{\dagger\ell} \frac{1}{\sqrt{Z_{diag}}} R_m^\dagger R_m \ell_{can} \\ &\equiv \bar{\ell}_{eign-m} M_{diag} \ell_{eign-m}. \end{aligned} \quad (\text{B.23})$$

Here we find how to get the final diagonal mass basis lepton after considering one loop effects:

$$M_{diag} = R_m \frac{1}{\sqrt{Z_{diag}}} R^\ell M_{ji} R^{\dagger\ell} \frac{1}{\sqrt{Z_{diag}}} R_m^\dagger \quad (\text{B.24})$$

$$\ell_{eign-m} = R_m \sqrt{z_{diag}} R^\ell \ell. \quad (\text{B.25})$$

Now we can finally show how one loop effects make non diagonal charged interactions:

$$-\frac{g}{\sqrt{2}} \bar{\ell} \not{W}^- Z^W \nu + h.c. = -\frac{g}{\sqrt{2}} \bar{\ell} \not{W}^- R_m \frac{1}{\sqrt{Z_{diag}^\ell}} R^\ell Z^W R^{\dagger\nu} \frac{1}{\sqrt{Z_{diag}^\nu}} \nu_{can} + h.c. \quad (\text{B.26})$$

$$Z^W = R_m \frac{1}{\sqrt{Z_{diag}^\ell}} R^\ell Z^W R^{\dagger\nu} \frac{1}{\sqrt{Z_{diag}^\nu}} \quad (\text{B.27})$$

To make this relevant to the experiment we have to consider an amplitude containing creating a neutrino at the source and detecting it back in the detector. This amplitude will contain

$$\mathcal{M} \propto Z_{ki}^+ Z_{jk} = (ZZ^\dagger)_{ji} \quad (\text{B.28})$$

Where i and j are the indexes in the mass basis of the leptons. We thus find

$$\begin{aligned} (ZZ^\dagger)_{ji} &= R_m \frac{1}{\sqrt{Z_{diag}^\ell}} R^\ell Z^W R^{\dagger\nu} \frac{1}{\sqrt{Z_{diag}^\nu}} \frac{1}{\sqrt{Z_{diag}^\nu}} R^\nu Z^W R^{\dagger\ell} \frac{1}{\sqrt{Z_{diag}^\ell}} R_m^\dagger \\ &= R_m \frac{1}{\sqrt{Z_{diag}^\ell}} R^\ell Z^W (Z^\nu)^{-1} Z^W R^{\dagger\ell} \frac{1}{\sqrt{Z_{diag}^\ell}} R_m^\dagger \end{aligned} \quad (\text{B.29})$$

Finally, we note that we can define $\sqrt{Z}^{-1} = R^{\ell\dagger} 1 / \sqrt{Z_{diag}^\ell} R^\ell$, where \sqrt{Z}^{-1} is the matrix that gives $\Rightarrow (\sqrt{Z}^{-1})^2 = Z^{-1}$. Then we can redefine, $R^\ell \sqrt{Z}^{\ell-1} = 1 / \sqrt{Z_{diag}^\ell} R^\ell$. This gives,

$$(ZZ^\dagger)_{ji} \Rightarrow = R_m R^\ell \sqrt{Z}^{-1} Z^W (Z^\nu)^{-1} Z^{W\dagger} \sqrt{Z}^{-1} R^{\dagger\ell} R_m^\dagger. \quad (\text{B.30})$$

Since $Z = \delta + \epsilon$, (i.e. the diagonal term and the term from the loop corrections), then $Z^{-1} = \delta - \epsilon + \mathcal{O}(\epsilon^2)$ because we need $ZZ^{-1} = \delta$. Also, from the way we define the matrix \sqrt{Z}^{-1} we can clearly see that $\sqrt{Z}^{-1} = \delta - \epsilon/2 + \mathcal{O}(\epsilon^2)$. We finally arrive at the result from above:

$$\begin{aligned} (ZZ^\dagger)_{ji} &= R_m R^\ell \left(1 - \frac{\epsilon^\ell}{2} + \mathcal{O}(\epsilon^2) \right) (1 + \epsilon^W) (1 - \epsilon^\nu + \mathcal{O}(\epsilon^2)) (1 + \epsilon^{W\dagger}) \left(1 - \frac{\epsilon^\ell}{2} + \mathcal{O}(\epsilon^2) \right) R^{\dagger\ell} R_m^\dagger \\ &= R_m R^\ell R^{\dagger\ell} R_m^\dagger + R_m R^\ell \left(-\frac{\epsilon^\ell}{2} + \epsilon^W - \epsilon^\nu + \epsilon^{W\dagger} - \frac{\epsilon^\ell}{2} \right) R^{\dagger\ell} R_m^\dagger + \mathcal{O}(\epsilon^2) \\ &= \delta_{ji} + R_m R^\ell (\epsilon^W + \epsilon^{W\dagger} - \epsilon^\nu - \epsilon^\ell) R^{\dagger\ell} R_m^\dagger + \mathcal{O}(\epsilon^2) \end{aligned} \quad (\text{B.31})$$

As a final note we see from the amplitude that for the anti process we have $\mathcal{M} \propto Z_{ki} Z_{jk}^+ = (ZZ^\dagger)_{ji}^T$. Therefore, to observe CP violation we need $(ZZ^\dagger) \neq (ZZ^\dagger)^T$.

Therefore, Z has to be imaginary. This is a trivial statement that only phases can contribute to CP violation. In this case the phases are emergent from the effective operators and come out of the phases in the new physics.

B.3 Detailed calculation in a simplified model

Here we present an example of calculating correction to the kinetic term and interaction term in the MSSM.

B.3.1 loop correction for the kinetic term

Let us consider the mass correction of the charged leptons with one of the neutralinos in the loop. The matrix element is given by

$$\begin{aligned}
\delta K &= (-i)^2 2g'^2 g_Y^2 \sum_{kl} V_{ki} (-im_{kl}^2) V_{lj}^* \int \frac{d^4 k}{(2\pi)^4} \frac{(i)^3 \not{k}}{(k^2 - m_{\ell_l}^2)(k^2 - m_{\ell_k}^2)((p-k)^2 - m_\chi^2)} P_L \\
\delta K &= 2g'^2 g_Y^2 \sum_{kl} V_{ki} m_{kl}^2 V_{lj}^* \int \frac{d^4 k}{(2\pi)^4} 2 \iiint dx dy dz \delta(1-x-y-z) \\
&\quad \frac{\not{k}}{(k^2 - xm_{\ell_l}^2 - ym_{\ell_k}^2 + z(p^2 - 2k \cdot p) - zm_\chi^2)^3} P_L \\
&= 2g'^2 g_Y^2 \sum_{kl} V_{ki} m_{kl}^2 V_{lj}^* \int \frac{d^4 k}{(2\pi)^4} 2 \\
&\quad \times \iiint \frac{dx dy dz \delta(1-x-y-z) \not{k}}{((k - (1-x-y)p)^2 - xm_{\ell_l}^2 - ym_{\ell_k}^2 + (z-z^2)p^2 - zm_\chi^2)^3} P_L \tag{B.32}
\end{aligned}$$

then $\ell = k - (1-x-y)p$

$$\begin{aligned}
\ell \text{ odd} \Rightarrow \delta K &= 2g'^2 g_Y^2 \sum_{kl} V_{ki} m_{kl}^2 V_{lj}^* \not{p} \int \frac{d^4 \ell}{(2\pi)^4} 2 \iiint dx dy dz \delta(1-x-y-z) \\
&\quad \times \frac{z}{(\ell^2 - xm_{\ell_l}^2 - ym_{\ell_k}^2 + (z-z^2)p^2 - zm_\chi^2)^3} P_L \tag{B.33}
\end{aligned}$$

When we take this in comparison to the vertex, $\bar{v}_j / p Z_{ji} P_L v_i$, $Z_{ji} = \delta_{ij} + \epsilon_{ij}$, we find:

$$\begin{aligned}
(\delta K = /p\epsilon) \Rightarrow \epsilon_{ij} &= 2g'^2 g_Y^2 \sum_{kl} V_{ki} m_{kl}^2 V_{lj}^* \int \frac{d^4 \ell}{(2\pi)^4} 2 \iiint dx dy dz \delta(1-x-y-z) \\
&\quad \times \frac{z}{(\ell^2 - x m_{\ell_l}^2 - y m_{\ell_k}^2 + (z-z^2) p^2 - z m_\chi^2)^3} \\
\ell_E^0 = i\ell \Rightarrow \epsilon_{ij}(p \rightarrow 0) &= 4g'^2 g_Y^2 \sum_{kl} V_{ki} m_{kl}^2 V_{lj}^* \iiint dz dx dz \delta(1-x-y-z) z (-i) \\
&\quad \times \int \frac{d^4 \ell_E}{(2\pi)^4} \frac{1}{(\ell_E^2 + x m_{\ell_l}^2 + y m_{\ell_k}^2 + z m_\chi^2)^3} \\
\text{Polar coor.} \Rightarrow &= 4g'^2 g_Y^2 \sum_{kl} V_{ki} m_{kl}^2 V_{lj}^* \iiint dx dy dz \delta(1-x-y-z) z \left(\frac{1-i}{2} \frac{-i}{(2\pi)^4} \right) \\
\frac{1}{2} d\ell_E^2 = \ell_E d\ell_E & \\
&\quad \times \int d\Omega \int_0^\infty d\ell_E^2 \frac{\ell_E^2}{(\ell^2 + x m_{\ell_l}^2 + y m_{\ell_k}^2 + z m_\chi^2)^3} \\
&= \left(\frac{-i}{16\pi^2} \right) 2g'^2 g_Y^2 \sum_{kl} V_{ki} m_{kl}^2 V_{lj}^* \int_0^1 dx \int_0^{1-x} dz \\
&\quad \times \frac{z}{\left(x(m_{\ell_l}^2 - m_{\ell_k}^2) + z(m_\chi^2 - m_{\ell_k}^2) + m_{\ell_k}^2 \right)} \tag{B.34}
\end{aligned}$$

This gives:

$$\begin{aligned}
\mathcal{I}_{kl}^{(1-mass)} &= \left(\frac{-i}{16\pi^2} \right) 2g'^2 g_Y^2 \sum_{kl} V_{ki} m_{kl}^2 V_{lj}^* \left[\frac{m_\chi^2 (m_\chi^2 - m_{\ell_k}^2) (m_\chi^2 - m_{\ell_l}^2) (m_{\ell_k}^2 - m_{\ell_l}^2)}{2(m_\chi^2 - m_{\ell_k}^2)^2 (m_\chi^2 - m_{\ell_l}^2)^2 (m_{\ell_k}^2 - m_{\ell_l}^2)} \right. \\
&\quad \left. \frac{(m_\chi^4 m_{\ell_k}^4 - 2m_\chi^2 m_{\ell_k}^4 m_{\ell_l}^2) \log \frac{m_\chi^2}{m_{\ell_k}^2} + (m_\chi^4 m_{\ell_l}^4 - 2m_\chi^2 m_{\ell_l}^4 m_{\ell_k}^2) \log \frac{m_\chi^2}{m_{\ell_l}^2}}{2(m_\chi^2 - m_{\ell_k}^2)^2 (m_\chi^2 - m_{\ell_l}^2)^2 (m_{\ell_k}^2 - m_{\ell_l}^2)} \right. \\
&\quad \left. + \frac{m_{\ell_k}^4 m_{\ell_l}^4 \log \frac{m_{\ell_k}^2}{m_{\ell_l}^2}}{2(m_\chi^2 - m_{\ell_k}^2)^2 (m_\chi^2 - m_{\ell_l}^2)^2 (m_{\ell_k}^2 - m_{\ell_l}^2)} \right] \tag{B.35}
\end{aligned}$$

Let us see how this relates to the low Higgs mass limit: We take $m_k \rightarrow m_l$

$$\mathcal{I}_{kl}^{(1-mass)} \rightarrow \left(\frac{-i}{16\pi^2} \right) 4g'^2 g_Y^2 \sum_{kl} V_{li} m_{ll}^2 V_{lj}^* \frac{m_\chi^4 - m_{\ell_l}^4 - 2m_\chi^2 m_{\ell_l}^2 \log \frac{m_\chi^2}{m_{\ell_l}^2}}{4(m_\chi^2 - m_{\ell_l}^2)^3} \tag{B.36}$$

If we turn m_{kl}^2 to δ_{kl} then

$$\mathcal{I}_{kl}^{(1-mass)} \rightarrow \left(\frac{-i}{16\pi^2} \right) 4g'^2 g_Y^2 \sum_{kl} V_{li} V_{lj}^* \frac{m_\chi^4 - m_{\ell_l}^4 - 2m_\chi^2 m_{\ell_l}^2 \log \frac{m_\chi^2}{m_{\ell_l}^2}}{4(m_\chi^2 - m_{\ell_l}^2)^3} \quad (\text{B.37})$$

Our original Feynman diagram becomes proportional to $\frac{i}{-m_\ell^2} (-i\delta) \frac{i}{-m_\ell^2} = \frac{i}{m_\ell^4} = \frac{d}{dm_\ell^2} \left(\frac{i}{-m_\ell^2} \right)$, as we expect.

B.3.2 loop correction for the interaction vertex

Let us consider a correction to the interaction term $\ell_\ell \nu_k W$ with a neutralino running in the loop. To calculate the matrix element for the vertex with one mass insertion. We assume $p, p', q \ll k$ as we are developing this in the $p = 0$ limit.

$$i\mathcal{M}_{ij} = -i\sqrt{2}2gg'^2 q_Y^2 \sum_{kl} V_{ki} m_{\ell,kl}^2 V_{lj}^* \times \int \frac{d^4 k}{(2\pi)^4} \frac{k_\mu k}{(k^2 - m_{\nu_l}^2)(k^2 - m_{\tilde{l}_l}^2)(k^2 - m_{\tilde{l}_k}^2)(k^2 - m_{\chi^0}^2)} P_L \epsilon^\mu \quad (\text{B.38})$$

Therefore

$$\epsilon_{ij} = 4gg'^2 q_Y^2 \sum_{kl} V_{ki} m_{\ell,kl}^2 V_{lj}^* \mathcal{I}_{kl}^{(1-mass)} \quad (\text{B.39})$$

and with a cutoff

$$\mathcal{I}_{kl}^{(1-mass)} = \frac{-i}{d} \left(\frac{1}{16\pi^2} \right)_{4D} \int_0^\infty dk_E^2 \frac{k_E^4}{(k_E^2 + m_{\nu_l}^2)(k_E^2 + m_{\tilde{l}_l}^2)(k_E^2 + m_{\tilde{l}_k}^2)(k_E^2 + m_{\chi^0}^2)} \quad (\text{B.40})$$

This integral is finite and does not need a regulator,

$$\mathcal{I}_{kl} = \frac{-i}{d} \left(\frac{1}{16\pi^2} \right)_{4D} \times \left(\frac{m_\chi^4 \log m_c^2}{(m_\chi^2 - m_k^2)(m_\chi^2 - m_l^2)(m_c^2 - m_\nu^2)} + \frac{m_k^4 \log m_k^2}{(m_k^2 - m_\chi^2)(m_k^2 - m_l^2)(m_k^2 - m_n^2)} + \frac{m_l^4 \log m_l^2}{(m_l^2 - m_\chi^2)(m_l^2 - m_k^2)(m_l^2 - m_\nu^2)} + \frac{m_\nu^4 \log m_\nu^2}{(m_\nu^2 - m_\chi^2)(m_\nu^2 - m_k^2)(m_\nu^2 - m_l^2)} \right) \quad (\text{B.41})$$

Now the sneutrino masses to this order will be degenerate with the slepton masses. Since we contracted the sneutrino with the l 'th index will call the mass m_ℓ .

$$\mathcal{I}_{kl}^{(1-mass)} = \frac{-i}{d} \left(\frac{1}{16\pi^2} \right)_{4D} \int_0^\infty dk_E^2 \frac{k_E^4}{(k_E^2 + m_{\ell_l}^2)(k_E^2 + m_{\ell_l}^2)(k_E^2 + m_{\ell_k}^2)(k_E^2 + m_{\chi^0}^2)} \quad (\text{B.42})$$

After some algebra we get:

$$\begin{aligned} \mathcal{I}_{kl}^{(1-mass)} = & \frac{-i}{d} \left(\frac{1}{16\pi^2} \right)_{4D} \left[\frac{m_{\ell_l}^2 (-m_\chi^2 + m_{\ell_l}^2)(m_\chi^2 - m_{\ell_k}^2)(m_{\ell_l}^2 - m_{\ell_k}^2)}{(m_\chi^2 - m_{\ell_l}^2)^2 (m_\chi^2 - m_{\ell_k}^2)(m_{\ell_l}^2 - m_{\ell_k}^2)^2} \right. \\ & + \frac{m_\chi^4 m_{\ell_l}^2 (m_{\ell_l}^2 - 2m_{\ell_k}^2) \log \frac{m_\chi^2}{m_{\ell_l}^2} + m_\chi^4 m_{\ell_k}^4 \log \frac{m_\chi^2}{m_{\ell_k}^2}}{(m_\chi^2 - m_{\ell_l}^2)^2 (m_\chi^2 - m_{\ell_k}^2)(m_{\ell_l}^2 - m_{\ell_k}^2)^2} \\ & \left. + \frac{m_{\ell_l}^2 (-2m_\chi^2 + m_{\ell_l}^2) m_{\ell_k}^4 \log \frac{m_{\ell_l}^2}{m_{\ell_k}^2}}{(m_\chi^2 - m_{\ell_l}^2)^2 (m_\chi^2 - m_{\ell_k}^2)(m_{\ell_l}^2 - m_{\ell_k}^2)^2} \right] \quad (\text{B.43}) \end{aligned}$$

Let us see how this relates to the low Higgs mass limit: we take $m_k \rightarrow m_\ell, m_{ij}^2 = \delta_{ij}$ then,

$$\mathcal{I}_{kl}^{(1-mass)} \rightarrow \frac{-i}{d} \left(\frac{1}{16\pi^2} \right)_{4D} \left(-\frac{3m_\chi^4 - 4m_\chi^2 m_{\ell_l}^2 + m_{\ell_l}^4 - 2m_\chi^4 \log \frac{m_\chi^2}{m_{\ell_l}^2}}{2(m_\chi^2 - m_{\ell_l}^2)^3} \right) \quad (\text{B.44})$$

$$\begin{aligned} (d=4) \quad \epsilon = & -igg'^2 q_Y^2 \sum_k V_{ki} V_{kj}^* \frac{1}{2} \left(\frac{1}{16\pi^2} \right) \\ & \times \left(-\frac{3m_\chi^4 - 4m_\chi^2 m_{\ell_l}^2 + m_{\ell_l}^4 - 2m_\chi^4 \log \frac{m_\chi^2}{m_{\ell_l}^2}}{(m_\chi^2 - m_{\ell_l}^2)^3} \right) \quad (\text{B.45}) \end{aligned}$$

If we take the $Su(2)$ soft mass limit we find:

$$\begin{aligned}
\epsilon &= \sum_k (4g'^2 q_Y^2) V_{ki} V_{kj}^* \frac{1}{4} \frac{1}{16\pi^2} \left[\log \frac{\Lambda^2}{\mu^2} \right. \\
&\quad \left. + \frac{m_{\tilde{\nu}_k}^4 (m_\chi^2 - m_{\tilde{\ell}_k}^2) \log \frac{m_{\tilde{\nu}_k}^2}{\mu^2} + m_{\tilde{\ell}_k}^4 (m_{\tilde{\nu}_k}^2 - m_\chi^2) \log \frac{m_{\tilde{\ell}_k}^2}{\mu^2} + m_\chi^4 (m_{\tilde{\ell}_k}^2 - m_{\tilde{\nu}_k}^2) \log \frac{m_\chi^2}{\mu^2}}{(m_{\tilde{\nu}_k}^2 - m_{\tilde{\ell}_k}^2)(m_{\tilde{\nu}_k}^2 - m_\chi^2)(m_{\tilde{\ell}_k}^2 - m_\chi^2)} + \mathcal{O}\left(\frac{1}{\Lambda^2}\right) \right] \\
&\xrightarrow{m_{\tilde{\nu}_k}^2 \rightarrow m_{\tilde{\ell}_k}^2} \sum_k (g'^2 q_Y^2) V_{ki} V_{kj}^* \frac{1}{16\pi^2} \left[\log \frac{\Lambda^2}{\mu^2} \right. \\
&\quad \left. - \frac{m_{\tilde{\ell}_k}^2 (m_{\tilde{\ell}_k}^2 - m_\chi^2) + m_{\tilde{\ell}_k}^2 (m_{\tilde{\ell}_k}^2 - 2m_\chi^2) \log \frac{m_{\tilde{\ell}_k}^2}{\mu^2} + m_\chi^4 \log \frac{m_\chi^2}{\mu^2}}{(m_{\tilde{\ell}_k}^2 - m_\chi^2)^2} + \mathcal{O}\left(\frac{1}{\Lambda^2}\right) \right] \tag{B.46}
\end{aligned}$$

Thus, as we expect:

$$\begin{aligned}
\partial_{m_{\tilde{\ell}_k}} \epsilon &= \sum_k (g'^2 q_Y^2) V_{ki} V_{kj}^* \frac{1}{16\pi^2} \left[-\frac{3m_\chi^4 - 4m_{\tilde{\ell}_k}^2 m_\chi^2 + m_{\tilde{\ell}_k}^4 - 2m_\chi^4 \log \frac{m_\chi^2}{m_{\tilde{\ell}_k}^2}}{(m_{\tilde{\ell}_k}^2 - m_\chi^2)^3} \right. \\
&\quad \left. + \mathcal{O}\left(\frac{1}{\Lambda^2}\right) \right] \tag{B.47}
\end{aligned}$$